UNIVERSITEIT VAN PRETORIA
UNIVERSITY OF PRETORIA
YUNIBESITHI YA PRETORIA

Mesoporous Silica recovery from Phlogopite by *Aqua Regia* leaching

by

Iwouda Venter

A dissertation submitted in partial fulfilment
of the requirements for the degree

Master of Engineering (Chemical Engineering)

in the

Department of Chemical Engineering
Faculty of Engineering, the Built Environment and Information Technology

University of Pretoria
Pretoria

December 2015

Mesoporous Silica recovery from Phlogopite by *Aqua Regia* leaching

Iwouda Venter

CVD 800
2015 – 12 – 05

Mesoporous Silica recovery from Phlogopite by *Aqua Regia* leaching

IZ Venter

29073937

Department of Chemical Engineering

University of Pretoria

CVD 800
2015 – 12 – 05

Mesoporous silica recovery from Phlogopite by *Aqua Regia* leaching

Synopsis

Phlogopite is a mineral found in the Phalaborwa complex, which is mined in abundance and has little to no industrial use. Phlogopite in its raw form consists of between 40 – 50% silicon. Previous studies have yielded various forms of silica through acid leaching of phlogopite. The aim is to leach phlogopite with *aqua regia* to obtain mesoporous silica with the maximum specific surface area possible. Interest in mesoporous silica utilization has greatly increased in areas such as catalysis, polymer reinforcement, adsorption and medical uses.

Phlogopite is leached in a temperature controlled batch reactor with *aqua regia*, nitric acid and hydrochloric acid to recover the remaining silicon product. The leaching conditions are varied in order to obtain the silicon oxide with the largest specific surface area. The leaching conditions such as acid concentration, nitrate ratio, leaching time, temperature, solid to liquid ratio, stirring speed and particle size are varied to determine the effects on the surface area.

With *aqua regia* as leaching agent the maximum specific surface area of 99.41% silica achieved was 515 m^2/g at acid concentration of 8.40 M, nitrate ratio of 0.64, leaching time of 12 hrs and leaching temperature at 50 ˚C. This experiment provided mesoporous silica with average pore width of 2.62 nm and average pore volume of 0.36 cm^3/g. Similar specific surface area values were achieved with 6.33 M nitric acid, leaching time of 6 hrs and leaching temperature at 60 ˚C. A regression (R^2= 0.90) was developed which can accurately estimate the specific surface area of the recovered silica with the known acid concentration, nitrate ratio, leaching time and temperature.

Keywords: Phlogopite, *aqua regia*, surface area, acid leaching

Contents

Acronyms

M – Molar Concentration	mol/l
AC – Acid Concentration	M
T – Temperature	˚C
t – Time	hrs
SSA – Specific Surface Area	m^2/g
ρ – Density	g/cm^3

Nomenclature

NR – Nitrate Ratio

Ratio of nitrate ions in the *aqua regia* mixture of chloride and nitrate ions

$$NR = \frac{[NO_3^-]}{[NO_3^-] + [Cl^-]}$$

MR – Mass Recovery

Mass of remaining sample after leaching divided by the total original leaching mass

$$MR = \frac{Mass\ remaining\ after\ leaching\ (g)}{Original\ leaching\ mass\ (g)} * 100$$

1. Introduction

Background

Phlogopite is a mineral found in the Phalaborwa complex which currently has limited industrial uses. Phlogopite in its raw form consists of silicon, aluminum, magnesium, potassium and iron. Phlogopite has a typical chemical formula of $K(H_2O)_n[Mg_{3-x}Fe_x(Si_3Al)O_{10}(OH)_2]$ however, the exact chemical composition depends on the geology of the area from which it is mined (Wypych *et al*, 2004).

Phlogopite contains high amounts of silica typically between 40 – 50% on a mass basis. Silica has various forms depending on its composition, morphology and properties. All forms of silica have unique applications in everyday life. Crystalline silica is used as an adsorbent material in water purification systems and in polymers. Amorphous silicon oxide is generally used in the cores of optical fibers and is essential in silicon based metal oxide semiconductor devices. These silica products are used in multimillion rand industries which are continuously expanding, which create a definite need for silica.

Problem Statement

The problem is to best utilize the abundant amounts of phlogopite through acid leaching, to recover mesoporous silica with maximum specific surface area.

Objective Statement

The objective is to determine the leaching conditions capable of providing silica with the maximum specific surface area. Various leaching conditions such as acid type, acid concentration, nitrate ratio, leaching time, temperature, solid to liquid ratio, stirring speed and particle size affect surface area. Partial/full factorial experimental design procedures are used to determine optimal leaching conditions, decreases experimental variation and maximum experimental results.

Scope of Investigation

Phlogopite is leached in temperature controlled batch reactors, the acid type, acid concentration, nitrate ratio, leaching time, temperature, solid to liquid ratio, stirrer speed and particle size are varied in order to determine the combination capable of providing the maximum specific surface area of the silica residue.

2. Literature Review

2.1 Phyllosilicates

Phyllosilicates, also known as sheet silicates, form part of an important group of minerals which include micas, chlorite, serpentine, talc, etc. Phyllosilicates consist of groups of SiO_4^{4-} bonds arranged in a tetrahedral arrangements as shown in Figure 1 (Jordan, *sa;* Nelson, 2011).

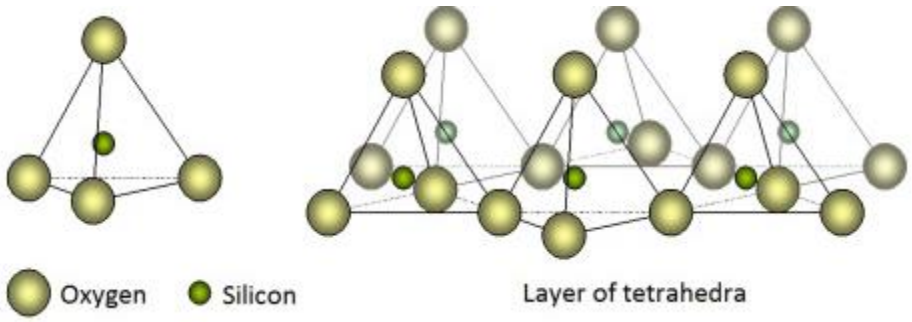

Figure 1: Tetrahedral SiO_4^{4-} arrangement

In the silicon – oxygen tetrahedral arrangement, the fourth vertex binds to a central cation in an octahedral (cation) layer. The cation layer is arranged in an octahedral arrangement as shown in Figure 2 (Jordan, *sa;* Nelson, 2011).

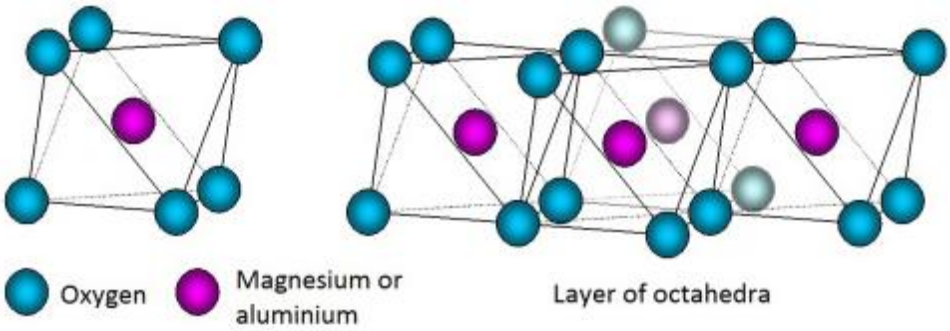

Figure 2: Octahedral arrangement of cations

The octahedral layer usually consists of Fe^{2+}, Mg^{2+} and Al^{3+}. A lamellar structure is formed by the bonding of tetrahedral – octahedral – tetrahedral (TOT) layers. Consequently the bonding between tetrahedral and octahedral

layers requires the sharing of O^{2-} or OH^- ions. In phyllosilicates the TOT layers are bonded together by Van der Waals forces. There are 2 groups of sheet silicates, namely trioctrahedral and dioctahedral sheet silicates. For trioctrahedral sheet silicates, each O^{2-} or OH^- ion is surrounded by 3 divalent cations, such as Mg^{2+} or Fe^{2+}. As for dioctahedral sheet silicates, each O^{2-} or OH^- ion is surrounded by 2 trivalent cations such as Al^{3+} or Fe^{3+} (Jordan, *sa;* Nelson, 2011).

2.2 Phlogopite

Phlogopite is a magnesium end member of the biotite group of micas. Mica in the biotite group is classified as phlogopite if the Mg:Fe ratio is larger than 2:1. Phlogopite generally has a Mg:Fe ratio larger than 5.3:1 (Aitta, Lajunen & Leskela, 1982). Phlogopite has a red – brown crystalline appearance. Phlogopite has a typical chemical formula as shown in Equation 1, however, the exact chemical formula depends on the geology of the area from where it is mined (Wypych *et al*, 2004).

$$K(H_2O)_n[Mg_{3-x}Fe_x(Si_3Al)O_{10}(OH)_2] \quad 1$$

Phlogopite has a typical TOT structure. The tetrahedral layers consist of repeating units of 4 O^{2-} ions bonded to Si^{4+} and Al^{3+} ions. The octahedral cation layer is occupied by di- and trivalent cations such as Al^{3+}, Mg^{2+}, Fe^{3+} and Fe^{2+} with minor traces of Mn^{2+}, Ti^{4+} and Li^{+} (Del Rey-Perez-Caballero & Poncelet, 2000). A singular octahedral metal layer is sandwiched in between 2 Si^{4+}/Al^{3+} tetrahedral sheets, forming a strong 3 sheet structure. Repeating TOT units are separated by an interlayer containing K^{+} (Harkonen & Keishi, 1984) as shown in Figure 3 (Phlogopite structure, *sa*). This structure is repeated up to a thousand times to form the layered crystalline structure of phlogopite.

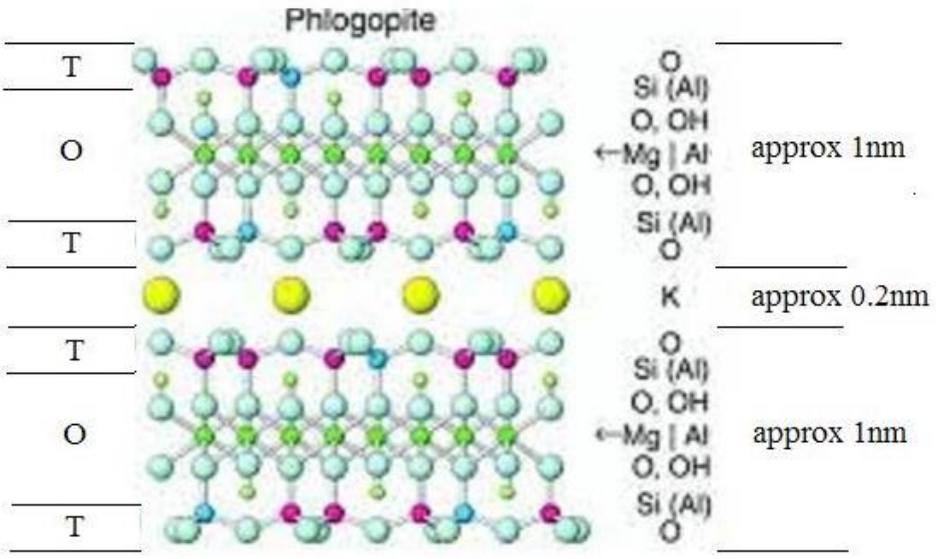

Figure 3: Structure of phlogopite

A single TOT – K layer has an approximately width of 1 nm (Harkonen & Keishi, 1984). The potassium interlayer is weakly bonded to the TOT structure by Van der Waals forces (Aitta *et al*, 1982). The potassium in the interlayer is easily removed through ion exchange of H^+ (from acids), resulting in easy separation of the layers forming smaller layered crystalline structures (Harkonen & Keishi, 1984). It is possible for phlogopite to have fluorine (replacing hydroxide) in the octahedral layers, increasing its resistance to weathering, hardness and thermal stability (Del Rey-Perez-Caballero & Poncelet, 2000).

Phlogopite can have numerous octahedral and tetrahedral ion substitutions which effect the chemical composition of the mineral. The Al^{3+} substitution of Si^{4+} in the tetrahedral layer is responsible for a charge deficiency resulting in a negative charge to the layer (Kaviratna & Pinnavaia, 1994). The K^+ ions are the dominant positive charge and are responsible for the charge neutralization between the unit layers. The unit layers are stacked in such a way that the K^+ ions are equidistant from 12 O^{2-} atoms – 6 O^{2-} ions from each tetrahedral layer. Phlogopite in its natural form does not swell when placed in water due to the hydration energy of the interlayer K^+ ion being insufficient to overcome the cooperative structural forces at the coherent edges of the surface (Del Rey-Perez-Caballero & Poncelet, 2000).

Repeating TOT structures are 0.2 nm apart resulting in phlogopite being regarded as a non – porous absorbent. The untreated phlogopite has a typical surface area of 1 m^2/g (Harkonen & Keishi, 1984). Phlogopite has very high dielectric characteristics, low hygroscopicity (ability to absorb or release water) and is an alkali resistant and thermal resistant electric-insulating material Phlogopite generally melts between 1400 – 1500 ˚C depending on the exact composition (Kraevskaya *et al*, 1985).

2.3 Leaching Agent (Lixiviant)

2.3.1 Hydrochloric Acid (Patnaik, 2007, 120)

Hydrochloric Acid (HCl) is one of the most corrosive non oxidizing strong acids. Hydrochloric acid is a colourless liquid, may cause severe burns to skin and irritate the respiratory system. Hydrochloric acid has a molecular weight of 36.46 g/mol and a boiling point range of 48 ˚C – 110 ˚C depending on the concentration. Hydrochloric acid is flammable and may produce hydrogen gas on prolonged contact with metals such as aluminum, tin, lead and zinc.

Hydrochloric acid is mainly used in industry for steel pickling, oil well acidizing, food manufacturing, producing calcium chloride and ore processing. Hydrochloric acid is also used for pH control, deionization of water and as a reducing agent.

2.3.2 Nitric Acid (Patnaik, 2007, 119)

Nitric acid (HNO_3) is a strong oxidizing agent which reacts violently and vigorously with numerous non – metallic substances. Nitric acid is a clear to yellowish liquid. Nitric acid may cause severe skin burns and respiratory tract irritation. Nitric acid has a molecular weight of 63.01 g/mol and a boiling point range of 86 ˚C – 122 ˚C depending on the concentration.

Nitric acid can result in an explosive reaction with metals except for precious metals, and is used for cleansing and assessing of precious metals. Depending on the reaction and dilution, nitric acid is highly corrosive and may dissolve many metals.

2.3.3 *Aqua Regia*

Aqua regia also known as royal water was discovered by an Arab alchemist, Jabir Ibn Hayyan in 720 – 813 AD. *Aqua regia* has the unique ability of dissolving gold and was extensively used in the 1890's for gold extracting from ore and it is still used for gold refinery today (Habashi, 2005).

Aqua regia is a strong oxidizing acid which consists of a mixture of hydrochloric acid (HCl) and nitric acid (HNO_3). It is a transparent – yellow liquid, is highly corrosive and has a pungent odour. *Aqua regia* has known catalytic activity, fumes in air and has an exothermic reaction when dissolved in water. *Aqua regia* typically consists of 2 – 3 volumes of concentrated HCl (36 – 38%) with 1 volume of concentrated HNO_3 (69 – 71%). It can however also be mixed on a 3:1 molar ratio of hydrochloric acid to nitric acid. *Aqua regia* is commonly used to remove noble metals such as gold, palladium or platinum in microfabrications and microelectronics. *Aqua regia* can also be used to wash glassware to remove organic compounds (Princeton University Aqua Regia, 2014).

Hydrochloric and nitric acid are both strong acids and strong electrolytes, which completely dissociate into ions. Both acids are monoprotic acids which dissociate once into the appropriate ions (Patnaik, 2007, 119 - 120). Hydrochloric acid will dissociate to hydrogen ions (H^+) and chlorine ions (Cl^-) and nitric acid will dissociate to hydrogen ions (H^+) and nitrate ions (NO_3^-). When hydrochloric acid and nitric acids are mixed the reactions takes place (Aqua Regia Decomposition, 2014) as shown in Equation 2 and Equation 3.

$$3HCl(aq) + HNO_3(aq) \rightarrow Cl_2(g) + NOCl(g) + 2H_2O(l) \qquad 2$$

$$2NOCl(g) \rightarrow 2NO(g) + Cl_2(g) \qquad 3$$

The reaction results in volatile product formation of nitrosyl chloride, chlorine and nitric oxide. This is characterized by the fuming nature and characteristic yellow colour of *aqua regia* (Aqua Regia Decomposition, 2014).

Nitrosyl chloride (NOCl) is a gas with an irritating odour. NOCl has major health hazards such as the ability to severely burn eyes, skins, respiratory tract and mucous membranes. NOCl can cause headaches, dizziness, difficulty to breath and lung congestion (Nitrosyl chloride Material Safety Data Sheet, 2008). The nitrosyl chloride dissociation is equilibrium limited, therefore fumes from aqua regia contain nitrosyl chloride, chlorine and nitric oxide (Aqua Regia Decomposition, 2014).

Chlorine gas (Cl_2) has a distinct irritating odour. Chlorine is harmful to inhale as it burns the respiratory tract and skin. Chlorine can rupture or explode containers if exposed to heat (Patnaik, 2007, 85)

Nitric oxide gas readily converts to nitrogen dioxide in air. Nitric oxide may irritate mucous membranes, sinuses, pharynx and bronchia and results in headaches and dizziness (Patnaik, 2007, 404)

2.4 Acid Leaching of Phlogopite

Various forms of phlogopite have been leached in numerous acids over the past years. The exact compositions of the phlogopite will depend on the geology of the ore body from which it is mined. Although the composition of phlogopite can vary slightly, the structure will remain the TOT mineral structure of repeating tetrahedral – octahedral – tetrahedral layers (Harkonen & Keishi, 1984).

Okada *et al* (2006) leached various phyllosilicates with TOT structures including phlogopite with H_2SO_4. The phlogopite was leached with 5 M H_2SO_4 for 1 – 10 hours at 70 ˚C. The maximum surface area obtained was 56 m^2/g. The leachability of TOT minerals by acids is strongly influenced by (Okada *et al*, 2006):

- The surface area
- Nature of octahedral cations
- Nature of tetrahedral cations
- Ratio of expandable sheets (leaching rate decreases with high Al^{4+} concentration in octahedral layer and low Al^{4+} concentration in tetrahedral layer)

Depending on the above variables the leaching rate of various minerals can be estimated. Vermiculite was used for comparison purposes due to its extensively recorded properties. Based on surface area and tetrahedral cations present, phlogopite should have a higher leachability than vermiculite but on the basis of octahedral cations present vermiculite should leach more readily than phlogopite. It is common to find talc and chlorite in the same area in which biotite as well as phlogopite and vermiculite are mined. Okada *et al* (2006) reported if these minerals are present in the phlogopite, these samples under prolonged leaching will become amorphous. Talc, chlorite and biotite require longer leaching due to their low leachability (Okada *et al*, 2006).

Harkonen & Keiski (1984) leached phlogopite from the Netherlands in nitric acid (HNO_3) hydrochloric acid (HCl) and sulfuric acid (H_2SO_4). They obtained

maximum surface areas of 620 m^2/g, 200 m^2/g and 190 m^2/g for HNO_3, HCl and H_2SO_4 respectively. They found that during leaching, the TOT structure expands. The tetrahedral silica tails on the edges of the structure become entangled and stay disordered during leaching. This results in pore formation between the 3 sheet structure and the entangled silicon oxide (SiO_4) tail ends – causing the surface area to increase from 1 m^2/g to several hundred m^2/g. Harkonen & Keiski (1984) found that the HNO_3 first dissolves the exchangeable K^+ ions from the interlamellar layer and then penetrates inwards to the Mg^{2+}, Al^{3+}, Fe^{2+} and Fe^{3+} cations in the octahedral layer.

Wypyth *et al* (2004) leached phlogopite from Brazil with nitric acid to investigate the distortion of the structure during leaching. They found that during acid leaching, ions from the interlayer and octahedral layer are removed first. There after the tetrahedral (silicon) layer distort, tilting bonds producing silanol groups (the silicon bonds previously bonded to the octahedral layer is now partly hydroxylated). This distortion results in the long range order of the structure to be lost resulting in an amorphous structure. However, the long range order can be reestablished causing the obtained silica to have a layered structure (Wypych *et al*, 2004).

Harkonen & Keiski (1984) tested the effect of thermal treatment on acid leached phlogopite. They noticed that thermal treatment of leached phlogopite at temperatures of 600 ˚C and 800 ˚C decreased the surface area by 20 % and 65 % respectively. They also investigated the effect of different sized particles and found that with a decrease in particle size the surface area increases from 218 m^2/g to 242 m^2/g and 256 m^2/g. Harkonen & Keiski (1984) discovered that by increasing the leaching temperature to 100 ˚C, the cation yield, surface area, average pore radius and amount of finer pores increased. The effect of acid concentration in their experiments yielded an increase in average pore radius with concentrated acid (5.71 M HNO_3) and less fine pores with weaker concentrations (0.83 M HNO_3) of acid. They also observed the total pore volume of HNO_3 leached phlogopite was much larger when compared to phlogopite leached with HCl and H_2SO_4.

To date there is no literature on acid leaching of phlogopite with *aqua regia*. However from the literature reviewed HNO_3 is a strong acid and strong oxidizing agent. It was also noted that phlogopite leached with HNO_3 provided a much higher SSA than HCl. *Aqua Regia* has 3 strong oxidizing agents, HNO_3, Cl_2 and NOCl. It is hypothesized these 3 strong agents, oxidize the cations to higher oxidation states increasing their affinity to react with the highly negative nitrate and chloride ions available. In turn resulting in mesoporous silica with higher SSA values

Currently industrial HNO_3 is priced between US $ 300 - 500 per ton (Price of Nitric Acid, sa) with the current exchange rate (R15.94/dollar) that equates to between R 4770 – 7950 per ton (Exchange Rate). Whereas industrial HCl is priced between US $200 – 350 per ton (Price of Hydrochloric Acid, sa) and with the current exchange rate that equates to R 3180 – 5565 per ton. On average HNO_3 is sold at R 6360 per ton and HCl at R 4373 per ton. It is theorized that *aqua regia* will be able to provide higher SSA than HNO_3 and HCl alone. It is theorized that by using *aqua regia*, less nitric acid will used decreasing the raw material costs of the process.

2.5 Acid Leaching Mechanism

There are primarily two methods for metal ion exchange in the octahedral layers – edge attack and gallery access as shown in Figure 4 (Harkonen & Keishi, 1984; Kaviratna & Pinnavaia, 1994).

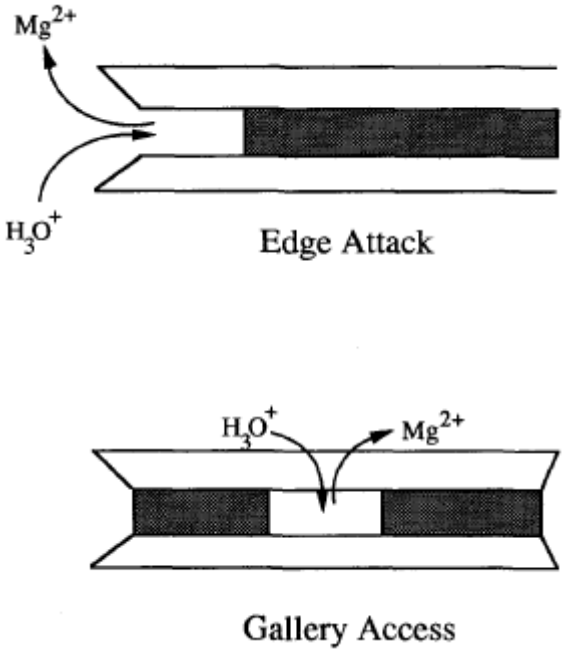

Figure 4: Edge attack and gallery attack

Phlogopite is classified as a TOT layered aluminosilicate non – swelling clay. The acid hydrolysis of swelling versus non swelling clays results in different physical and chemical properties. In general acid hydrolysis of swelling clays provides higher surface areas of the remaining silica structure than non-swelling clays (Kaviratna & Pinnavaia, 1994).

Kaviratna & Pinnavaia (1994) and Harkonen & Keiski (1984) experiments showed structural defects after acid leaching due to the dissolution of the octahedral cations. Kaviratna & Pinnavaia (1994) used X-ray diffraction (XRD) and determined the structural changes are due to edge attack as no indications of intragallery ion exchange.

From the XRD no peak broadening was seen, this is an indication that the preferred method of ion exchange is edge attack (Kaviratna & Pinnavaia, 1994). These results suggest that the ion exchange is much smaller than the rate of layer hydrolysis. Therefore the gallery attack pathway is unfeasible and the depletion of the Mg^{2+} from the octahedral layer is favored by proton attack at the edge layer (Kaviratna & Pinnavaia, 1994, Harkonen & Keishi, 1984).

Kaviratna & Pinnavaia (1994) reports a decrease in the surface area with an increase in Mg^{2+} deletion and reached a maximum surface area of 31 m^2/g at a Mg^{2+} depletion of 53%. They attempted to replicate the experiments of Harkonen & Keiski (1984), but were unable to reach the maximum surface area of 620 m^2/g. This can be explained by Kaviratna & Pinnavaia (1994) using 10.17 M HCl for 1 hour whereas Harkonen & Keiski (1984) used 5.71 M HNO_3 for 168 hours.

Kuwahara and Aoki (1995) investigated the dissociation process by acid leaching phlogopite with a solution of 0.01 M HCl containing 0.1 M NaCl. They investigated the effect of temperature, leaching time and acid volume. With an increase in temperature an increase in dissociation was achieved. This provides a maximum metal removal from the octahedral layer however this also includes Si^{4+} removal from the tetrahedral layer. This is unfavourable as we want to remove as much metal ions as possible while retaining the maximum Si^{4+} ions for highest surface area. This same trend is also seen for the leaching interval. As the leaching interval extends more Si^{4+} is removed, this results in destruction of tetrahedral sheets.

Kuwahara and Aoki (1995) reports the priority of phlogopite dissociation for 100 ml HCl as $K^+ > Fe^{3+} > Mg^{2+}$, $Al^{3+} > Si^{4+}$. This is however, not seen in a 20 ml samples. The smaller leaching solution with the longer leaching period selectively removes more Si^{4+}. From their experiments, their best results were achieved at higher temperatures with larger leaching volume and a moderate leaching period. A summary of experiments that reported the highest surface areas are shown in Table 1.

Table 1: Maximum surface area reported from literature

Acid Type	Concen-tration (M)	Tempera-ture (˚C)	Leaching Time (hours)	Particle Size Average (µm)	Solid/Liquid Ratio (g/ml)	Surface Area (m^2/g)	Additional Comments	References
HNO_3	5.71	25	168	550		620		Harkonen & Keiski, 1984
HNO_3	5.71	100	0.33	550		616		Harkonen & Keiski, 1984
HNO_3	5.71	25	72	550		592		Harkonen & Keiski, 1984
HNO_3	5.71	25	72	550		592	Thermal treatment at 150˚C for 16h	Harkonen & Keiski, 1984
HNO_3	5.71	25	72			586		Harkonen & Keiski, 1984
HNO_3	5.71	25	72			584	Thermal treatment at 300˚C for 16h	Harkonen & Keiski, 1984
HNO_3	5.71	100	0.17			508		Harkonen & Keiski, 1984
HNO_3	0.83	100	5			398		Harkonen & Keiski, 1984
HCl	5.71	100	5			198		Harkonen & Keiski, 1984
H_2SO_4	5.71	100	4			189		Harkonen & Keiski, 1984
H_2SO_4	5.00	70	2		1.5/75	56		Okada *et al*, 2006
H_2SO_4	5.00	70	1		1.5/75	52		Okada *et al*, 2006

2.6 Kinetics of Acid Leaching of Phlogopite

Malmstrom & Banwart (1997) suggested the weathering of micas, in which the structure and compositions are changed, is generally altered in the following steps:

- Exchange of K^+ by a hydrated ion resulting in expansion of the interlayer spacing
- Decrease in Al^{3+} substitution in the tetrahedral layer, increasing the Si^{4+}/Al^{3+} ratio, reducing the layer charge
- Due to expansion of interlayer, enhanced cation exchange capacity (CEC)
- Substitution of divalent ions by trivalent ion in the octahedral layer
- Oxidation of divalent iron

Malmstrom & Banwart (1997) investigated the dissolution of biotite dependency on pH and stoichiometry. They report congruent steady state dissolution rate of Fe^{3+}, Mg^{2+}, Al^{3+} and Si^{4+} near a pH of 2 (0.01M). In a pH range of 4 – 7 (1×10^{-4}M – 1×10^{-7}M) the preferential release of metals changed into a preferential silicon release, indicating a strong dissociation dependency on pH. They suggest that the dissociation reaction is surface reaction controlled, with adsorption of protons at low pH while higher pH increases dissociation and favours desorption of protons.

Malmstrom & Banwart (1997) noted that under acid conditions, the release of metal ions in the octahedral layers (Fe^{3+}, Mg^{2+} and Al^{3+}) is favoured. Between 10 – 15 days the release of octahedral metals are the same as the release of tetrahedral Si^{4+}, resulting in congruent dissociations. The reverse was observed for basic to neutral pH ranges. For basic and near neutral pH values, the release of octahedral metals are favoured, followed by a preferential release of Si^{4+}.

From the experiments performed by Malmstrom & Banwart (1997) it is reported that the removal of ions from the structure is independent of the time scale of the experiment. It was also seen that metals are released in nonstoichiometric ratios. They explain these observations with 2 possible scenarios:

- Irreversible nonstoichiometric release due to the mineral
- Congruent dissociation of the biotite with re-adsorptions of the removed ions resulting in either formation of additional mineral or the re-adsorption into the leaching mineral.

Lin & Clemency (1981) studied the dissolution kinetics of phlogopite. They found that the use of pH buffers and washing of the phlogopite before dissociation has a great effect on the end result. By making use of a buffer to control the pH of the dissociation solution, the presence of very small quantities of K^+ (in the leaching medium) will decrease the release of K^+ from the interlayer of Phlogopite. They reported washing the raw phlogopite to remove fine particles can result in great cations losses even though organic solvents are used.

Lin & Clemency (1981) used carbon dioxide (CO_2) as a buffer in order not to contribute any organic or inorganic ions which could influence the dissociation process. Upon the addition of the CO_2, the solution pH increased rapidly from 3.78 to 5.11 in 3 minutes. After the 1010 hour experiment only 0.95% Mg^{2+}, 0.74% Fe and 0.54% Si^{4+} had been removed from the original phlogopite – the result can be attributed to high pH values as a result of insufficient acid addition. This dissociation suggests the release of Si^{4+} will be the rate limiting step in the dissociation reaction. This release of Si^{4+} will also be the rate of the destruction of the tetrahedral sheets – which could possibly form a protective layer around the remaining mineral structure which will affect the dissociation rate.

2.7 Potassium Extraction

Potassium is removed from the interlayer of phlogopite through acid leaching or ion exchange. It is known that the presence of certain cations such as K^+, Cs, Rb and NH_4 in the extraction liquid may delay the removal of potassium from the interlayer (Mamy, 1969). Mamy (1969) investigated the observation by adding small amounts of $NaNO_3$ to $Ca(NO_3)_2$ and $Ca(NO_3)_2$ to HNO_3 to determine the effect of the addition of Na^+ and H^+ on the K^+ exchange.

Mamy (1969) found that with the addition of $NaNO_3$ to $Ca(NO_3)_2$,there was a greater release of K^+ from the interlayer. This addition of a second cation (Na^+) of low normality did not greatly affect the chemical properties of the $Ca(NO_3)_2$. In relation to cationic charges, for the replacement of one K^+ only one Na^+ is needed whereas for the replacement of one Ca^{2+} two K^+ are needed. This clearly indicated the replacement of one Ca^{2+} requires less energy than the replacement of two Na^+ in the interlayer. They described the K^+ replacement in the interlayer to be due to hydration which increases the interlayer distance. For layered silicates (phlogopite) the hydration states of divalent cations are more stable than for monovalent cations. This suggests that the Na^+ may be used in order to initiate new exchange cycle of the following order, Na^+ exchange with K^+ and Ca^{2+} exchange with Na^+.

When the $Ca(NO_3)_2$ is added to HNO_3, an increase in K^+ removal is observed. With the addition of $Ca(NO_3)_2$ to HNO_3 the K^+ release drastically increased. This observation suggests the Ca^{2+} and K^+ exchange is dependent on the prior H^+ and K^+ exchange. Mamy (1969) observed with higher H^+ concentration, more of the octahedral lattice is dissolved, releasing the cations more readily.

Ross and Rich (1973b) investigated the effect of particle size on K^+ removal of phlogopite. They related the phlogopite particle size to the particle thickness, due to layer expansion being responsible for the K^+ removal or sorption. They performed 2 day experiments where previously reacted phlogopite was added to fresh $CaCl_2$ and left to react for another 2 days. This process was repeated for a

total of 14 days (7 experiments consisting of 2 days each). From their results, maximum K^+ removal was achieved within 2 days of treating phlogopite with $CaCl_2$. The results suggest within the first set of 2 day experiments the finer particles with the smallest thickness, has the highest K^+ exchange. However after the first 2 day experiment the larger particles with thicker layers had higher K^+ exchange capabilities. They suggest the thicker particles are capable of further bending of the TOT layers, providing higher K^+ exchange capacity, whereas the layers of thinner particles tend to split instead of bending, resulting in higher K^+ selectivity decreasing the K^+ exchangeability.

Ross and Rich (1973a) suggest the degree of K^+ depleted phlogopite as well as particle size will affect the resorption of K^+ into the phlogopite. Large particles are able to release and resorb larger amounts of K^+ than small particles. It is suggested that large particles are more capable of marginal expansion than smaller particles, this expansion allows more K^+ to either be released or resorbed. The marginal expansion allows the TOT layers to bend and rotate which results in higher K^+ release. This results in more energy needed to split layers in larger particles than in smaller particles, allowing more K^+ to be removed of resorbed before the collapse of the interlayers. They investigated the effect of K^+ depletion in conjunction with particle size, their results suggest larger particles with complete K^+ depletion have higher K^+ sorption rate than smaller particles with partial K^+ depletion.

2.8 Silica

Silica is also known as silicon dioxide (SiO_2). Various forms of silica naturally exits such as quartz, cristobalite, stishovite, coesite and tridymite. Silica can also be synthetically made, by leaching Phlogopite with acid. The heavy metals within the phlogopite structure is removed and the remaining solid residue is silicon dioxide. Silica has a crystallographic structure where silicon molecule is tetrahedrally bonded to oxygen atoms. Silica minerals generally have strong structures which fail in a brittle manner under imposed stress. Pure silica minerals are transparent in colour while pure silica powder is white in colour (Steward & Simmons, 2015).

Silica has numerous uses for example in construction, ceramics, glass, fillers for paint and rubber, desiccant in medical field, water filtration, anti - foaming agent, carrier material in chemistry, stabilizer and adsorbent materials. The application of the silica depends on its composition and molecular structure. Silica can either be crystalline or amorphous in structure depending on the formation process and conditions. Silica has a density range of 1.8 – 4.3 g/cm^3 and surface area values range of 2 – 2000 m^2/g (Iler, 1979: 19). The exact surface area of a particle is dependent on its size, lattice distortion and pores within the particle. Particles can have macro, meso or micropores. Particles with macropores have pores with diameter greater than 50 nm, mesoporous particles have pores sized between 2 and 50 nm and micropore particles have pores sized less than 2nm (Iler, 1979: 7).

2.8.1 Crystalline Silica

Crystalline silica can either be anhydrous or hydrated crystalline silica.

2.8.1.1 Anhydrous Crystalline Silica’s

The most well known form of anhydrous crystalline silica is quartz (sand), however other forms of crystalline silica are widely used. Crystalline silicas

that are thermodynamically stable at low pressures are quartz, tridymite and cristobalite. As the pressure increases other forms of silica such as keatite, coesite and stishovite became thermodynamically stable (Iler, 1979: 15). The pressure to temperature relationships of the crystalline silica can be seen in Figure 5.

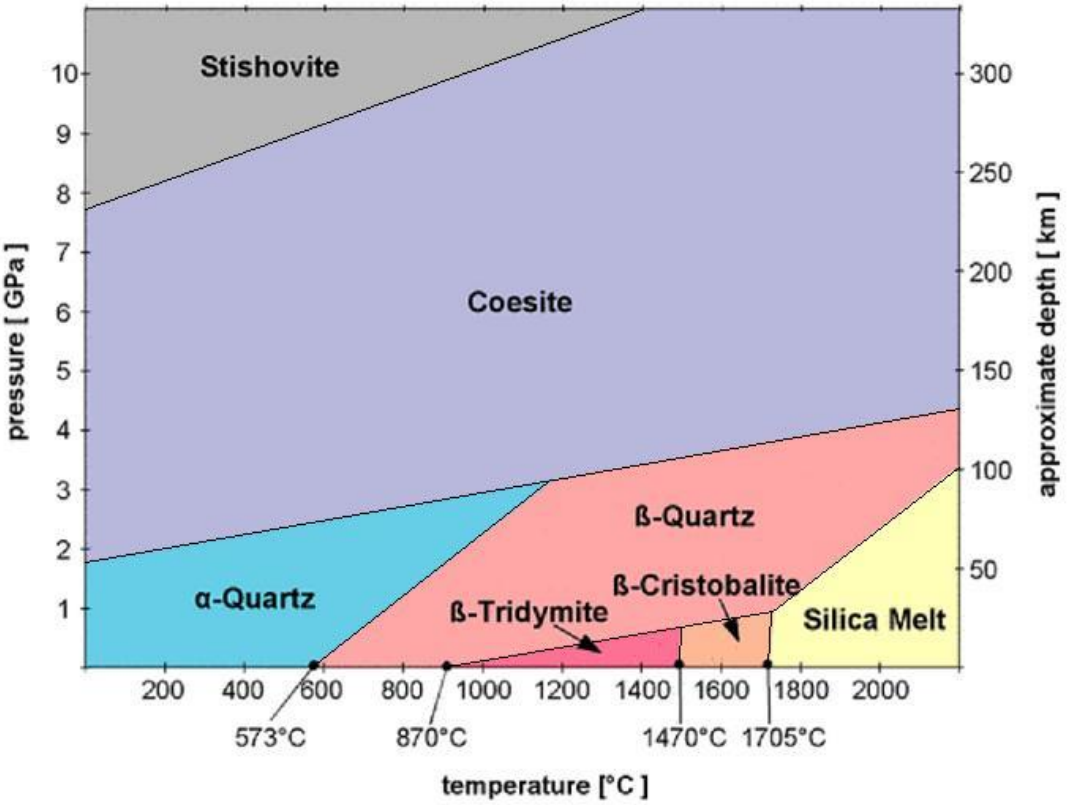

Figure 5: Phase diagram of crystalline silica (Akhaven, 2014)

The properties and structural differences of these different phases of silica have been well investigated and published. Along with these common phases there are unusual anhydrous crystalline forms such as Silica W, melanophlogite, Silica O and silicate. Silica W has a fibrous crystalline silica structure with an average density of 1.97 g/cm³. It is formed in the gas phase by oxidizing silicon monoxide vapours at elevated temperatures around 1200 – 1400 ˚C before forming paper like films. Silica W is stable in dry air however is converted into amorphous hydrated silica by moisture, while still remaining in its swollen fibrous form. Melanophlogite is known as a cubic polymorph of silica with a very open structure. Melanophlogite typically consists of 92.40% SiO_2 and 5.70% SO_3 and has a density of approximately 2.05 g/cm³. If heated and the

volatile components are removed the density decreases to 1.99 g/cm³. The pores in the silica are lined with oxygen which is greatly hydrophobic and organophilic (Iler, 1979: 18).

2.8.1.2 Hydrated Crystalline Silica's

It is well known that definite crystalline structure have been recovered by the extraction of cations from crystalline silicates with the use of acid. However there is no occurrence of a hydrated crystalline structure forming from a silica and water solution. However there have been cases where certain hydrates formed show sign of characteristic solubility which suggests that equilibrium is achieved. This equilibrium suggests that if silica changes from solid phase to solution the reverse where silica changes from solution to solid phase must hold (Iler, 1979: 20).

Lepidoidal silica is silica which forms extremely small flakes or scales and can be crystalline of amorphous. These silicates are usually hydrated depending on process of how they are formed. These flakes have internal hydrogen bonds and have a weak acidity. Three types of common lepidoidal silicates are:

- Synthetic silica ($[(Si_6O_6)O_3](OH)_6$) prepared from siloxane obtained by the hydrolysis of calcium silicide
- Sheet like forms of silica by extracting layer – type basic copper silicate with acid
- Flake like gel made by freezing solutions of colloidal silica

Although these hydrated silicas have very similar physical forms they differ greatly in structure (Iler, 1979: 20).

2.8.2 Amorphous Silica

Amorphous silica can generally be divided into three groups:

- Vitreous silica – formed by fusing quartz

- Silica M – amorphous silica formed by either amorphous or crystalline silicas through radiation with high speed neutrons. The density of the crystalline silica decreases and the density of the amorphous silica increases. Silica M typically has a density of 2.26 g/cm³ which is close to the density of vitreous or microamorphous silica with a density of 2.20 g/cm³
- Microamorphous silica – which include gels, powders and porous glass. These generally have particles smaller than a micron meter in size and have a surface area larger than 3 m²/g

Amorphous silica is not completely amorphous but rather consists of extremely small regions of crystallinity. Even so the XRD (X-Ray Diffraction) analysis of an amorphous sample shows a broad band instead of multiple characteristic peaks. Microamorphous silica occurs in nature or can be made in a laboratory. In the laboratory microamorphous silica can be divided into the three groups:

- Microscopic sheets, ribbons and fiberlike formed from a customized process.
- Commonly formed spherical amorphous particles of SiO_2 less than a 0.1 μm in diameter. The surface of these spherical particles consists of either anhydrous SiO_2 or SiOH groups. These spheres can either be linked together in three – dimensional arrangements or stand separately.
- Hydrated amorphous silica, where the silicon atoms are attached to one or more hydroxyl groups, retaining the hydroxyl groups in the silica structure. This type of silica is obtained if silicic acid is concentrated in a water system, the mixture easily polymerizes at low temperature in acid conditions. The polymerized silica form extremely small spheres with diameters of approximately 20 – 30 Å (0.002 – 0.003 μm), which bond together to form 3 dimensional gel structures (Iler, 1979: 22).

These microamorphous structures often collapse when the solution temperatures are higher than 60 ˚C or if the pH of the solution is not kept in acid conditions.

2.8.3 Silica Solubility

Solubility data of silica below a temperature of 150 ˚C differs greatly depending on the trace amounts of metals impurities, the structure of the silica (amorphous or crystalline) or if the surface of the silica is disturbed or not. With the use of electron diffraction it was found that quartz has a thin layer of amorphous silica or disturbed layers of silica on its surface. The disturbed layer of silica is in the form of "mosaic" silica consisting of colloidal sized silica particles. The amorphous layer is typically 100 Å (0.01 μm) thick. The amorphous layer or disturbed layer of a crystalline quartz particle can be removed by the use of dilute, typically 9 – 15% Hydrogen Flouride (HF) while washing for approximately 5 min. Further inspections reveal these disturbed layers can be up to 2 μm in width, when aged in water. When the disturbed layer is removed, the underlying structure will return to a normal crystalline structure. After cleaning the silica surface (removing the amorphous or disturbed layer) typical crystalline solubility at 25 ˚C ranges from 6 – 11 ppm (Iler, 1979: 31).

The dissolution of crystalline silica proves to be very complex. It was found that solubility in terms of dynamic equilibrium between silica in solution and silica in solid phase only exists with crystalline quartz and amorphous silica. The dissolution of silica in water occurs rapidly once the silica is introduced to the water, thereafter the dissolution decreases until equilibrium is reached. When the crystalline silica is suspended in water, the final silica solution concentration is saturated. This observation is only noticed for crystalline quartz and amorphous silica. For other forms of crystalline silica the final silica concentration on solution depends on the $Si(OH)_4$ transfer from solid to solution and vice versa, the re - adsorption of $Si(OH)_4$ increases rapidly onto the surface decreasing any further dissolution (Iler, 1979: 37).

Amorphous silica has a higher solubility in water than crystalline silica. Reported solubility values for amorphous silica range from 70 – 150 ppm at 25 ˚C. The variation in solubility is dependent on particle size, internal hydration and presence of impurities either in the silica structure or on the silica surface. Determination of equilibrium for silica is highly time consuming due to continuous $Si(OH)_4$ dissolution and re–adsorption to and from the solution to

the solid silica. Therefore depending on the state of the surface of the amorphous silica, before being dried the number of hydroxyl groups per unit surface area differs greatly. The surface state of the dried silica then affects the solubility. In general, when amorphous silica is placed in water at 25 ˚C the pH greatly affects the solubility. At pH values below 7, the soluble silica concentrations increase over several days and advances to the final equilibrium value asymptotically. At pH values above 7, the silica concentration in solution increases rapidly with in the first 24 hours reaching a supersaturated solution, there after the concentration decreases in the next 3 – 4 days and reaches the characteristic solubility of the pH. During the first 24 hours the rate of dissolution is far greater than the rate of deposition, resulting in a supersaturated silica solution at higher pH values (Iler, 1979: 41).

Since the surface of amorphous silica differs drastically the exact solubility values at a given pH and temperature are difficult to determine. However at 25 ˚C the solubility of amorphous silica varies from 70 – 180 ppm. As the temperature increases the solubility increases as expressed in Equation 4

$$\log C = \frac{-731}{T} + 4.52 \qquad 4$$

Where C is mg SiO_2/kg (ppm) and T is the absolute temperature. However the maximum temperature is 200 ˚C, as above this temperature amorphous silica crystallizes rapidly (Iler, 1979: 45).

The effect of particles size on the solubility of silica in water was also investigated. It was found that if the surface of the silica is convex the solubility is higher compared to that of a concave surface. This observation is dependent on the radius on the curvature and the larger the radius the smaller the effect on solubility. Therefore for smaller particles the radius of curvature is smaller resulting in higher equilibrium solubility. An important practical consequence is that when two or more smaller particles coagulate, at the point of contact the radius of curvature is extremely small and the solubility of silica

in the contact region is very small. Silica then dissolves from the silica surface and deposits on the contact point of the particles (Iler, 1979: 50).

2.9 Summary

A qualitative summary of the conditions needed for leaching of phlogopite with aqua regia to obtain the maximum surface area is shown in Table 2.

Table 2: Qualitative summary of conditions

	Parameter	Condition	Comments
1	Nitrate Ratio (NR) $(NO^-_3/(NO^-_3 + Cl^-))$	Unknown	No information about this parameter gained from literature, however from individual acids results, want more HNO_3 than HCl (Section 2.5)
2	Acid Concentration (AC)	Higher H^+ concentration	From literature want high concentration, however too high concentration could theoretically destroy the remaining silica structure (Section 2.6)
3	Leaching Time (t)	Higher	Theoretically the longer leaching period will remove more cations and provided a cleaner silica product – however if leaching period is too long, silica structure will break down (Section 2.6 & 2.7)
4	Leaching Temperature (T)	Higher	Theoretically the higher the leaching temperature the faster the leaching rate (Temperature dependency of Arrhenius rate equation)
5	Particle size	Larger	From basic engineering principles – the smaller the particle the faster the leaching. From literature the larger the particle the greater the cation removal
6	Solid to liquid ratio	Small	From literature the more liquid (acid) volume used the faster and better the cation removal (Section 2.5)
7	Stirring Speed	Unknown	Phlogopite leached via edge attack, reaction is diffusion controlled (Section 2.5)

3. Theoretical Background

3.1 Acid Leaching

3.1.1 Leaching Theory (Hydrometallurgy Theory and Practice, 2006; Levenspiel, 1999)

Leaching involves the dissolution of components from a mineral, concentrate or other intermediate product. The active chemical species responsible for the dissolution is known as the leaching agent or lixiviant. Typical leaching agents include sulfuric acid, sodium cyanide, hydrochloric acid or sodium hydroxide.

The terms leaching and dissolution have two distinct different implications however these terms are used interchangeably. Leaching usually refers to small fractional removals of a component of the total mass, whereas, dissolution involves high fractional removal (80 – 90%) of the total mass of a component. Different types of leaching include metal salt dissolution, acid/base reactions, ion exchange reactions, oxidative dissolution and reductive dissolution.

In order to determine the thermodynamic possibility of a leaching reaction, most commonly a Pourbaix diagram (voltage potential (E_H) versus pH diagram) for the species is considered. With the use of an E_H versus pH diagram the most appropriate conditions in determining the optimum leaching conditions for maximum recovery without dissolving large amount of unwanted ions can be theoretically determined.

3.1.2 Leaching Kinetics (Hydrometallurgy Theory and Practice, 2006; Levenspiel, 1999)

Kinetics of leaching reactions is focused around the rate limiting step in the reactions. The rate limiting step can be governed by the following:

- Mass transfer of the leaching agent from the bulk solution to the particle surface
- Mass transfer of the products away from the particle surface
- Mass transfer within the pores to the surface of the material
- Mass transfer within the reaction product layer around the particle
- Chemical reaction at the particle surface

The type of rate limiting step is dependent on the particle and the leaching agent. The type of kinetic module used to simulate the leaching reaction is also dependent on the properties of the particle, for example, for a non – porous solid being dissolved in a leaching agent, the shrinking core model is most likely used.

Activation energies of the leaching reactions can be an indication of the type of limitations of the reaction. If the activation energy is generally lower than 20 – 25 kJ/mole the reaction will be mass transfer controlled. Where the activation energy is in excess of 40 kJ/mol the reaction is chemical reaction rate controlled. This is a highly reliable method for determining whether the reaction is mass transfer controlled or chemical reaction controlled; however, this assumption is not necessarily conclusive.

The particle size or particle size distributions also play an important role in the reaction kinetics of a leaching reaction. When a group of particles are present with various particle size distributions, in a batch reactor, the different size distributions will be leached at different time intervals and will therefore have different residence times. In some cases the chemical reactivity is dependent on the initial size of the particles and can result in morphological changes due to the leaching reactions resulting in particle size varying with the extent of reaction.

3.1.3 Leaching Models (Levenspiel, 1999)

Heterogeneous reactions in which liquid reacts with solids, generally follow the reaction:

$$A(aq) + bB(s) \rightarrow leachate + solid\ products$$

For noncatalytic reactions with particles surrounded by fluids there are two well known models: the progressive – conversion model and the shrinking unreacted core model.

3.1.3.1 Progressive – Conversion Model (PCM)

For the PCM, the fluid enters and reacts throughout the particle. The reactions occur at different rates at different locations within the particle. Therefore the solid is converted to product constantly and gradually, as shown in Figure 6.

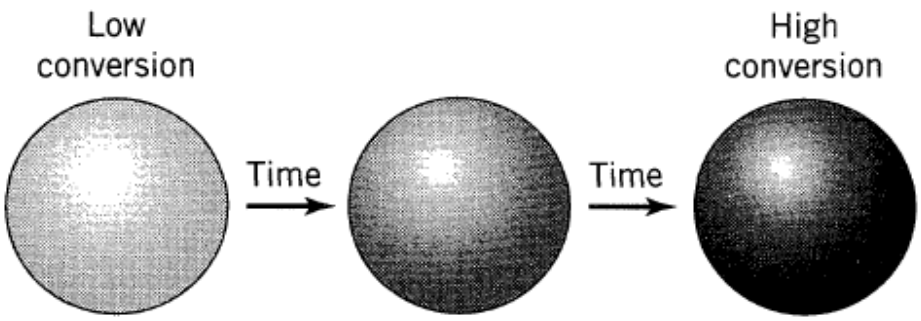

Figure 6: Progressive – conversion model

3.1.3.2 Shrinking – Core Model (SCM)

For the SCM, the reactions first takes place at the surface of the particles and thereafter progresses into the solids. The reaction leaves behind the converted product material as well as unreacted solids (ash). The SCM reaction pattern is shown in Figure 7.

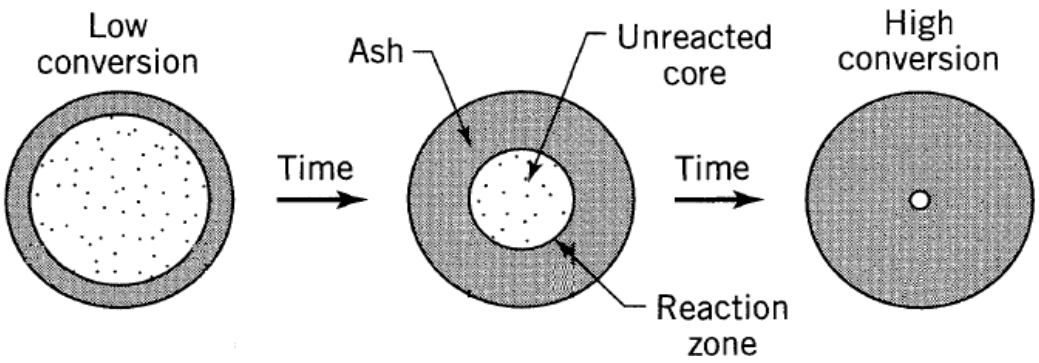

Figure 7: Shrinking core model

Comparing the Progressive – Conversion Model and the Shrinking – Core Model, the SCM closely resembles real life situations.

The SCM was first developed by taking into consideration the rate limiting steps (pg 9) and is shown in Figure 8

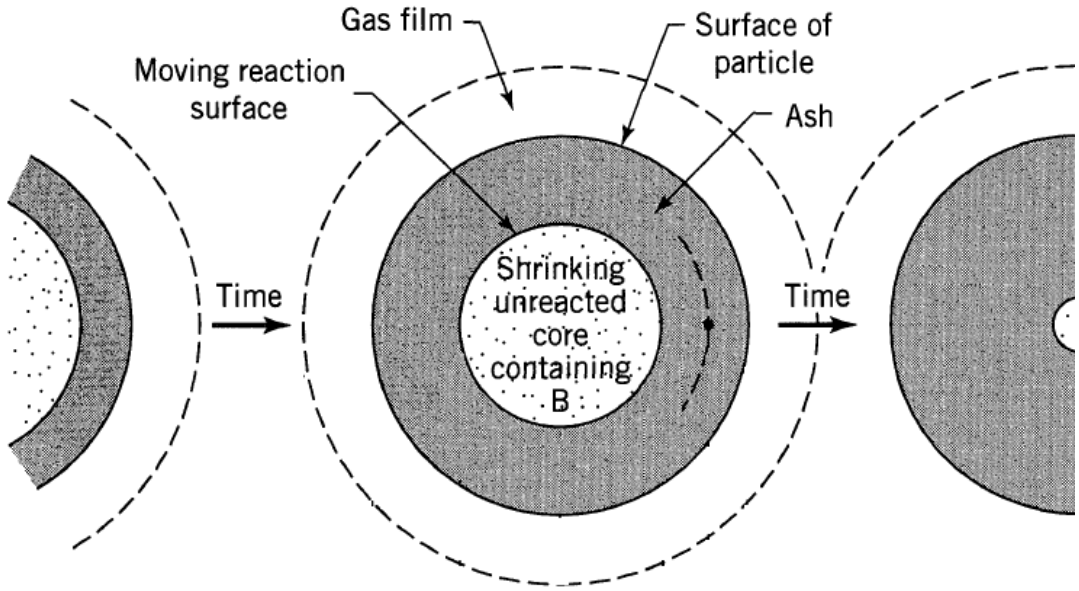

Figure 8: Reaction mechanisms considered in SCM development

The mechanisms shown in Figure 8 can be explained in the 5 steps:

1. Diffusion of reactant A through the film surrounding the particle to the surface of the solid.
2. Penetration and diffusion of A through blanket of ‘ash’ to the surface of the unreacted core

3. Reaction of A with solid (B) at this reaction surface
4. Diffusion of product through the 'ash' back to the exterior surface of solid
5. Diffusion of product through film back into the main body of fluid

In many reactions not all these steps exist, for example if no products are formed steps 4 and 5, do not contribute directly to the resistance to the reaction. The SCM was developed assuming steps 1, 2 and 3 are rate – controlling.

The kinetic equation derived for step 1, the diffusion of reactant A through film surrounding the particle to the surface of the solid, is shown in Equation 5

$$-\frac{1}{S_{ex}}\frac{dN_B}{dt} = bk_g\left(C_{Ag} - C_{As}\right) \qquad 5$$

Where S_{ex} is the exterior surface of the particle, $N_B$is the moles of the particle (B), t is the time, b is the stoichiometry constant for solid, k_g is the mass transfer coefficient between the fluid and the particle, C_{Ag} is the concentration of A in the gas (fluid) phase. The concentration driving force $C_{Ag} - C_{As}$ becomes C_{Ag} and is constant at all times in the reactions because C_{As} is the concentration of A at the particle surface and there is no fluid reactant at the particle surface.

The kinetic equation derived for step 2, penetration and diffusion through the ash layer is shown in Equation 6

$$-\frac{dN_A}{dt} = 4\pi r^2 \mathfrak{D}_e \frac{dC_A}{dr} \qquad 6$$

Where N_A is the mole of fluid (A), r is the radius of the spherical particle, $\mathfrak{D}_e$ is the effective diffusion coefficient of fluid in the ash layer and C_A is the concentration of A.

The kinetic equation derived for step 3, chemical reaction controlled is shown in Equation 7

$$-\frac{1}{4\pi r_c^2}\frac{dN_A}{dt} = bk''C_{Ag} \qquad 7$$

Where r_c is the radius of the unreacted core of the solid and k'' is the first – order rate constant for the surface reaction.

After integration and manipulation of the above equations, the time to reach any stage of conversion is as shown in Equation 8

$$t_{total} = t_{film\ alone} + t_{ash\ alone} + t_{reaction\ alone} \qquad 8$$

Similarly the estimation for complete conversion (τ) is shown in Equation 9

$$\tau_{total} = \tau_{film\ alone} + \tau_{ash\ alone} + \tau_{reaction\ alone} \qquad 9$$

The individual reaction time and conversion estimations for spherical and flat particles are shown in Table 3.

Table 3: Conversion estimations and reaction times

	Spherical particles	**Flat particles**	**Nomenclature**
Film Diffusion	$t = X_B\tau$ $X_B = 1 - \left(\frac{r_c}{R}\right)^3$ $\tau = \frac{\rho_B R}{3bk_g C_{Ag}}$	$t = X_B\tau$ $X_B = 1 - \frac{1}{L}$ $\tau = \frac{\rho_B L}{bk_g C_{Ag}}$	t – time τ – conversion L – half thickness R – radius ρ_B – bulk density
Ash Diffusion	$t = \left(1 - 3(1 - X_B)^{\frac{2}{3}} + 2(1 - X_B)\right) * \tau$ $\tau = \frac{\rho_B R^2}{6b\mathfrak{D}_e C_{Ag}}$	$t = X_B^2\tau$ $\tau = \frac{\rho_B L^2}{2b\mathfrak{D}_e C_{Ag}}$	$\mathfrak{D}_e$ – Effective Diffusion
Reaction Controlled	$t = 1 - (1 - X_B)^{\frac{1}{3}}) * \tau$ $\tau = \frac{\rho_B R}{bk'' C_{Ag}}$	$t = X_B\tau$ $\tau = \frac{\rho_B L}{bk'' C_{Ag}}$	k'' – first order rate constant for surface reaction

3.2 Factorial Experimental Design

Factorial Experimental design (FED) uses specially developed tables known as "orthogonal arrays". The use of orthogonal arrays allows easy and consistent experimental design. The orthogonal arrays are designed in such a way as to minimize deviation in experimental results due to uncontrollable environmental factors. Depending on the number of parameters changed during the experiments, the size of the orthogonal array can be determined. Once the size of the array is known the minimum number of experiments needed to be performed is known. The orthogonal arrays are designed in order to perform the minimum amount of experiments while still obtaining the maximum information available.

The FED has many advantages ranging from determining the optimal conditions of a process, consistency in experimental design and result analysis, drastic reduction in project time and cost of experiments, design of a robust process and by improvement of the design and process design and development (Roy, 1990: 17). The allure of the FED far outweighs its limitations. The only limitation of the FED is the timing at which it is applied, the only way the FED can be effective is if it is applied early in the research and development phase of a product of process.

There are 2 types of FED the Full Factorial Experimental Design (FFED) and the Partial Factorial Experimental Design (PFED). The most used orthogonal array is the L_8 (Table 4). The L_8 is used to design experiments with maximum 7 parameters each at 2 parameter levels. With the L_8 for the FFED, 3 parameters (columns) are assigned resulting in the remaining 4 columns being used to determine all the possible interactions between the parameters. With the L_8 PFED, 4 or more parameters (columns) are assigned resulting in the remaining columns being used to determine certain possible interactions.

Table 4: L_8 Orthogonal Array

	Parameters						
Number of Experiments	**P1**	**P2**	**P3**	**P4**	**P5**	**P6**	**P7**
1	-1	-1	-1	-1	-1	-1	-1
2	-1	-1	-1	1	1	1	1
3	-1	1	1	-1	-1	1	1
4	-1	1	1	1	1	-1	-1
5	1	-1	1	-1	1	-1	1
6	1	-1	1	1	-1	1	-1
7	1	1	-1	-1	1	1	-1
8	1	1	-1	1	-1	-1	1

Once the L_8 has been performed the results are analyzed using analysis of variance (ANOVA), main parameter effects and possible interactions plots. The ANOVA is a standard statistical technique used to determine the measure of confidence. Together with the ANOVA analysis multiple data regression is used to analyze the data. The linear data regression assists in the formulation of an empirical equation using the various parameters of the experiments to predict the outcome of a specific measured variable as shown in Equation 10 (Montgomery & Runger, 2007: 436)

$$y = \beta_0 + \sum_{i=1}^{7} \beta_i x_1 \qquad 10$$

where β is the coefficient for each experimental parameter x_1. With the regression the p value is determined. The p value is used to report the result of hypothesis testing in which the hypothesis is accepted or rejected at a specific level of significance. Therefore p values are defined as the smallest level of significance that would lead to rejection of the null hypothesis with the given data (Montgomery & Runger, 2007: 300). Hypothesis testing can be used in conjunction with confidence intervals. The use of p values and confidence intervals are used because they provide much more information than hypothesis

testing alone. For example hypothesis testing says whether the null hypothesis is accepted or rejected and the p value gives a numerical indication of the level of significance. Therefore using a 95% confidence interval if the p value is smaller than 0.05 the null hypothesis is rejected and the parameter is statistical significant (Montgomery & Runger, 2007; 302). After an initial FED has been performed and analyzed, an indication of which parameters are significant and whether the regression is linear or not can be determined. If the regression is not linear and there is expected curvature in the regression plot, the center and star points of the experiments are performed as shown in Table 5. To determine the position of the star points an alpha value (α) is introduced. The alpha value indicated the distance from the center point (0) where the star points have to be performed in order to maximize the information from the response area. For a L8 FED α is accepted as 1.4. The combination of the FED, center and star point's results can be used to determine a mathematical equation which predicts the results from the parameters in the form as shown in Equation 11

$$y = \beta_0 + \sum_{i=1}^{n} \beta_i x_i + \sum_{i=1}^{n} \sum_{j=1}^{n} \beta_{ij} x_{ij} + \sum_{i=1}^{n} \beta_{ii} x_i^2 \qquad 11$$

Table 5: Centre and star point's experimental designs

		Parameters			
	Number of Experiments	**P1**	**P2**	**P3**	**P4**
Centre Points	**9**	0	0	0	0
	10	0	0	0	0
Star Points	**11**	-α	0	0	0
	12	+α	0	0	0
	13	0	-α	0	0
	14	0	+α	0	0
	15	0	0	-α	0
	16	0	0	+α	0
	17	0	0	0	-α
	18	0	0	0	+α

3.3 Analysis Methods

3.3.1 Surface Area – BET

The specific surface area (SSA) of the samples were measured with the Micromeretics TriStar II Surface Area and Porosity BET. These tests are generally completed under cryogenic conditions, typically with liquid nitrogen (-195.8 ˚C) at one atmosphere pressure. The adsorption theory used is the BET (Brunauer, Emmett and Teller) theory. The BET incorporates the Langmuir theory with the concept of multimolecular layer adsorption (Webb *et al*, 1997: 62).

3.3.2 Density – Pycnometer

Density is measured with a pycnometer. The sample densities were measured in the Micromeritics AccuPyn II 1340 Gas Pycnometer. Helium gas pycnometers are much more accurate, easier to use and prove faster results then water based pycnometers.

3.3.3 Chemical composition – XRF

X – ray Fluorescence (XRF) is used to provide a quantitative analysis of the elements in a sample. The Thermo Fisher ARL Perform'X Sequential XRF with OXSAS software was used for analyses. The samples are dried at 100°C and roasted at 1000°C to determine Loss On Ignition (LOI) values.

3.3.4 Structural Morphology – XRD

X – Ray Diffraction (XRD) is a well-known method for determining the structure of complex samples. XRD provides a method to qualitatively identify different crystalline compounds. The XRD also provides an indication of whether the sample has a crystalline or amorphous structure (Skoog, Holler &

Crouch, 2007 :326). The samples were prepared according to the standardized Analytical backloading system, which provides nearly random distribution of the particles. They were analyzed using a PANalytical X'Pert Pro powder diffractometer in θ–θ configuration with an X'Celerator detector and variable divergence- and fixed receiving slits with Fe filtered Co-Kα radiation (λ=1.789Å). The phases were identified using X'Pert Highscore plus software.

3.3.5 Physical Morphology – FEG SEM

The Field Emission Gun Scanning Electron Microscope (FEG SEM) is a technique used to obtain details information about the physical appearance of a sample. The information is obtained through electron microscopy. The FEG SEM provides clear images with resolution down to 1 nm with ultra-high magnification imaging (Skoog, Holler & Crouch, 2007 :608). The samples were inspected with the use of a Zeiss Ultra Plus FEG SEM from Germany.

4. Experimental

4.1 Apparatus

The experiments were performed in temperature controlled batch reactors. The experimental setup consists of a water bath with a circulator and a water replacement system. The temperature controlled water bath is placed on top of magnetic stirrer plates which provide continuous mixing.

4.2 Planning

With the use of the literature survey, the independent variables such as acid concentration (AC), nitrate ratio (NR), leaching time (t), temperature (T), particle size, solid to liquid ratio and stirring speed are investigated. The choices of independent variables are chosen as justified from the literature survey as summarized in Section 2.10. For this study the nitrate ratio (NR), mass recovery (MR) and metal removal (M^+ rec) is defined as shown in Equation 12, 12 and 13, respectively. Thus for pure HNO_3 the NR = 1 and for pure HCl the NR = 0.

$$NR = \frac{[NO_3^-]}{[NO_3^-] + [Cl^-]} \quad 12$$

$$MR = \frac{Mass\ remaining\ after\ leaching\ (g)}{Origional\ leaching\ mass\ (g)} \quad 13$$

$$M^+rec = \frac{Cation\ Oxides\ remaining\ in\ leached\ sample}{Cation\ Oxide\ in\ origional\ sample} * 100 \quad 14$$

The quantity of cation oxides of leached samples were determined with the use of XRF, which provided the elemental concentrations in the samples. These concentrations were used to determine the $M^{+}rec$.

Preliminary experiments over a wide range of values were performed in order to narrow down the range in which the maximum specific surface area of the residual silica was achieved. The preliminary experiments ranges are as follows:

- AC: 0.97, 1.21, 3.07, 3.24, 4.20, 5.38, 8.21, 11.30 M
- NR: 0.23 0.43, 0.64, 0.73
- T: 30, 40, 50, 60, 70 ˚C
- t: 24, 48, 72, 96 hrs
- Particle size: 250 – 500 µm and 500 – 750 µm
- Solid to liquid ratio: 10g/200ml, 20g/200ml, 10g/400ml, and 20g/400ml
- Stirrer Speed: 370, 530, 690 and 855 rpm

From the results of the preliminary experiments, the following parameters were kept constant in all the experiments at the conditions that provided the maximum surface area values:

- Particle size: 250 – 500 µm
- Solid to liquid ratio: 20g/200ml
- Stirrer Speed: 530 rpm

The results from the preliminary experiments narrowed the ranges of the leaching conditions that provided the highest specific surface area values to:

- AC: 2.18 and 6.33 M
- NR: 0.56 and 0.73
- T: 40 and 60 ˚C
- t: 6 and 18 hrs

These leaching conditions were used in the full factorial experimental design (FFED) for HNO_3 and HCl as shown in Table 7 and Table 10. The leaching experiments were performed with pure HNO_3 and HCl in order to test the end

points of the NR ranges (0 and 1). These leaching conditions were also used for the PFED for *Aqua Regia* Exploratory as shown in Table 11. From the results of the HNO_3, HCl and *Aqua Regia* Exploratory experiments, the leaching conditions were changed accordingly for *Aqua Regia* Final.

- AC: 4.26 and 8.40 M
- NR: 0.47 – 0.64
- T: 50 and 70˚C
- t: 12 and 24 hours

The main dependent variable is the specific surface area (SSA) of the recovered silica determined by 5 point BET. Surface area values give an indication of available area for possible reaction sites; in general high surface area is associated with higher reactivity. Remaining dependent variables include density, mass recovery, composition (XRF) and crystalline structure (XRD and FEG SEM).

4.3 Method

The experiments are designed according to FFED and PFED and were performed in random order. *Aqua regia* is mixed according to the required acid concentration and acid ratio set in the FFED and PFED. The experimental procedure is as follows:

1. Wash and dry glassware and set water bath temperature to required leaching temperature
2. Calibrate pH meter
3. In a fume hood with appropriate safety equipment, use measuring cylinder to measure required volume of acids, for *Aqua Regia*, first measure HCl and pour into 500 ml Erlenmeyer flask, add HNO_3 to HCl slowly.
4. Measure pH of acid solution
5. Weigh 20 g of the 250 – 500 µm sized phlogopite
6. Add phlogopite to acid mixture
7. Gently insert magnetic stirrer bar to Erlenmeyer flask

8. Gently place weighed rings over flask and place in water bath, noting time, date, and water bath temperature.
9. Set magnetic stirrer plates to set stirring speed of 530 rpm
10. Place pH probe into distilled water to 'equalize' then place probe into probe container gently

After the required leaching time, the flask was carefully removed from the water bath. The weighted rings and the magnetic stirrer bar was removed from the flask. The following washing procedure was then followed in a fume hood:

1. Measure the pH of the solution
2. Carefully pour the reaction solution into 500 ml acid resistance centrifuge containers
3. Centrifuge the solution for 5 min at 2000 rpm
4. Using a syringe carefully take a sample of the acid solution and seal in a clearly marked container.
5. Carefully pour the remaining of the acid solution into a container without disturbing the silica residue.
6. Distilled water, 200 ml, is added to the silica residue in the centrifuge contained. The mixture is shaken to loosen the silica from the container.
7. The distilled water/silica solution is centrifuged for 5 min at 2000 rpm in order to remove any excess acid from the silica
8. The pH of the solution is measured
9. The liquid is carefully poured into a contained without disturbing the silica residue
10. Step 6 to 9 is then continuously repeated until a pH of 4 is reached. A pH of 4 is needed as it is the lowest threshold in order to analyze the silica in XRF, XRD, pycnometer, FEG SEM and BET.
11. The washing process uses approximately 2.4 l of distilled water per experiment in order to achieve a pH of 4 or higher.
12. The silica is placed in a petri dish and dried in a vacuum oven at 100 ℃ for 24 hours.
13. Neutralize acid mixture with

4.4 Quality Control and Quality Assurance

Raw Material Storage

The phlogopite was stored in sealed plastic sample bags and were placed in temporary locked storage when not used. The acids were locked inside a chemical store in between leaching intervals. General housekeeping principles were used to ensure clean and uncontaminated glassware before each use.

Experiment Preparation

For each leaching experiment, identical experimental procedure was followed. The same temperature control system, including water bath, water circulator and water replacement system was used. The same magnetic stirrer plates and stirrer bars were used to ensure consistency throughout each experiment. The same experimental method was used each time as discussed in Section 4.3 and the experiments were performed in random order.

Sample Collection and Analysis

The samples were collected after the silica residue was dried in a vacuum oven. The samples were stored in clearly labelled sealable plastic sample bags. Constant record was kept of each leaching experiment performed. The samples were temporarily stored in a locked unit until analyzed.

The samples were analyzed using various methods. The specific surface area values were measured using the standardized 5 point surface area determination procedure for silica using the Micromeretics TriStar II Surface Area and Porosity BET. During analysis, 5 SSA values were determined for the sample and an average was reported as the SSA. The densities of the samples were determined with the same Micromeritics AccuPyn II 1340 Gas Pycnometer, with 5 helium purges of the samples. The density of the sample was measured 5 times and the average value was reported. For FEG SEM inspection, the samples were coated twice with carbon to improve electron diffraction detection by the Zeiss Ultra Plus FEG SEM. The XRF analysis and sample preparation were performed by qualified personal using the THermo Fisher ARL Perform'X

Sequential XRF. The XRD analysis and sample preparation was performed by qualified personal using the PANalytical X'Pert Pro Powder diffractometer.

5. Results and Discussions

5.1 Phlogopite

Phlogopite was characterized using various techniques. The phlogopite was analyzed with the FEG SEM to closely inspect its layered platelet morphology as shown in Figure 9.

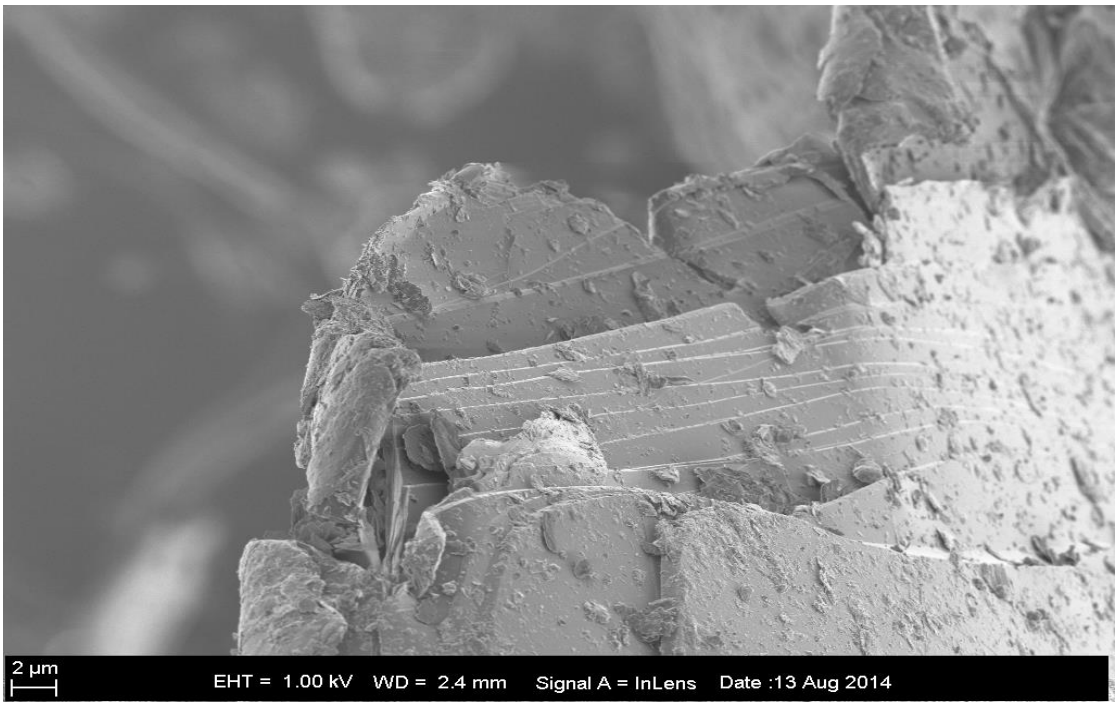

Figure 9: Layered phlogopite morphology as seen by FEG SEM images

The phlogopite samples were analyzed with XRD. The diffractogram contained well known characteristic peaks of phlogopite verifying its identification (according to X'Pert Highscore plus software) as shown in Figure 10.

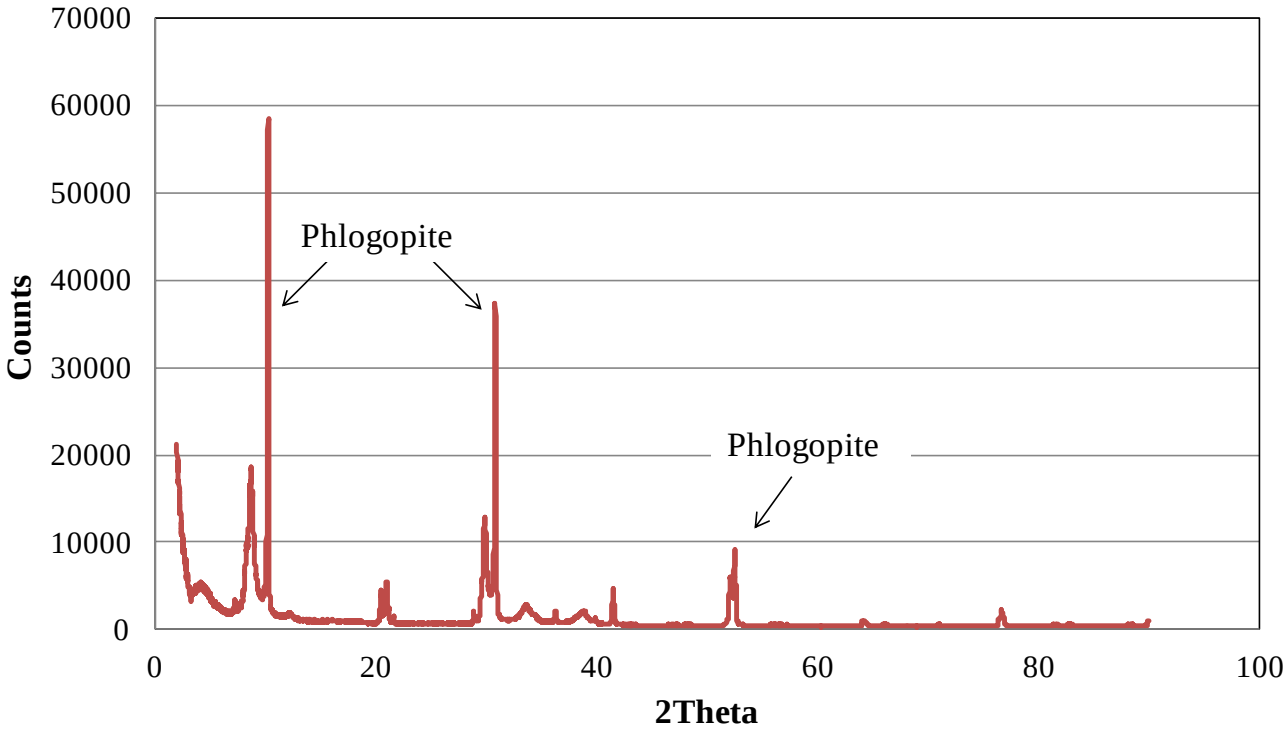

Figure 10: XRD of phlogopite with its characteristic identification peaks

Numerous Phalaborwa complex phlogopite samples were analyzed with XRF, the average composition values are shown in Table 6. The average measured specific surface area and density values are also shown in Table 6.

Table 6: Chemical Analysis of Phlogopite

%	**Phlogopite**
Sample	**Average**
SiO_2	41.72
MgO	25.45
Al_2O_3	10.11
Fe_2O_3	7.53
K_2O	7.13
TiO_2	0.66
Surface Area (m^2/g)	2.17
Density (g/cm^3)	2.69

The average specific surface area of phlogopite was measured to be 2.17 m^2/g with BET and the measured SSA value is similar to the average value obtained

in literature of 1 m²/g. The phlogopite samples density were determined with the use of a helium pycnometer to the average value of 2.69 g/cm³.

Foster (1960) developed a method for estimating the structural formula of trioctrahedral micas (phlogopites, biotites, siderphyllites and lepidomelanes) from the detailed results of the XRF analysis (Table 6). The structural formula is estimated by using the XRF analysis to determine the cations per unit cell and octahedral and tetrahedral layer charges. The structural half-cell formula was estimated to be as shown in Equation 15

$$\underbrace{[(Ti_{0.05}Fe^{3+}_{0.22}\,Mg_{2.70}\,Mn_{0.002})}_{2.97}\,(Si_{2.97}Al_{0.85}Fe^{3+}_{0.18})O_{10}\,(OH)_2]^{-1.00}\;(K_{0.65}Ca_{0.05})^{+0.70}_{0.70} \qquad 15$$

A range of experiments with varying conditions were performed in Nitric Acid, Hydrochloric Acid, *Aqua Regia* Set A and Set B. The individual factorial experiments are discussed before the combined results are presented and discussed.

From the results of the exploratory experiments performed as discussed in Section 4.2, the following parameters were kept constant for all the experiments:

- Solid to liquid ratio: 20g/200ml
- Particle Size: 250 – 500 µm
- Stirrer Speed: 530 rpm

5.2 Nitric Acid

The full factorial experimental design (FFED) for the leaching of phlogopite with nitric acid is shown in Table 7.

Table 7: Full Factorial Experimental Design for Nitric Acid

Number	**AC (M)**	**t (hrs)**	**T (˚C)**	**SA (m^2/g)**	**MR (g/g)**	**ρ (g/cm^3)**
N1	2.18	6	40	46	88.00	2.56
N2	2.18	18	40	188	76.60	2.29
N3	2.18	6	60	374	54.45	2.08
N4	2.18	18	60	490	47.10	2.04
N5	6.33	6	40	202	75.55	2.33
N6	6.33	18	40	378	55.15	1.97
N7	6.33	6	60	517	45.75	1.95
N8	6.33	18	60	460	45.20	2.01

The 2 highest specific surface area (SSA) values achieved by leaching phlogopite with nitric acid are 517 m^2/g (N7) and 490 m^2/g (N4). The nitric acid leached phlogopite samples with the largest SSA values were achieved at the higher leaching temperature of 60 ˚C. Harkonen & Keiski (1984) leached phlogopite, from Finland, with nitric acid and the most relevant results are shown in Table 8. When compared, the results obtained in Table 7 and Table 8 are similar. The highest SSA value was obtained from N7 of 517 m^2/g with leaching conditions of 6.33 M, 6 hrs at 60 ˚C. Harkonen & Keiski (1984) achieved surface area of 396 m^2/g at 5.71 M, 5 hrs at 100 ˚C from nitric acid leaching. They also achieved a SSA of 508 m^2/g at 5.71M, 0.33 hrs at 100 ˚C This significant difference in SSA values at similar acid concentrations suggest a highly significant dependency of SSA on leaching time and temperature. Nitric acid is a strong acid due to its low pKa value of -1.6. The pKa value indicates the acid's affinity for complete dissociation. Nitric acid is well known as a strong oxidizing agent, these characteristics are fundamental to its excellent leaching capability. Nitric acid is capable of removing 99.5% of the cations and 100% of the potassium from phlogopite rendering pure silica (Harkonen & Keiski, 1984).

Table 8: Harkonen & Keiski (1984) results for phlogopite leaching with nitric acid

Number	**AC (M)**	**t (hrs)**	**T (˚C)**	**SA (m^2/g)**	**K% Recovery**	**Cation % Recovery**
1	5.71	0.17	100	508	100	99.50
2	5.71	0.33	100	616	100	99.50
3	5.71	5	25	218	79	56.00
4	5.71	5	100	396	100	99.50
5	0.83	5	100	398	95	77.00
6	5.71	24	25	435	88	77.00
7	5.71	72	25	592	99	98.00
8	5.71	168	25	620	100	99.00

The MR of each leaching experiment was recorded as shown in Table 7, the results indicate as the MR decrease the SSA increases. As the MR decreases more cations are removed from the structure, an increase in vacant pores are available and the larger the measured SSA of the silica. The removal of cations, increase the number of vacant pores in the structure, significantly increasing the SSA from 2.17 to 517 m^2/g (N7) yielding a 237 times SSA increase. The XRF analysis reveals on average SiO_2 accounts for 41.72% of the total mass of the sample, therefore as the MR approaches 41.72%, more cations are removed increasing vacant pores available and the higher the SSA. The density values indicate the same trend as seen with the MR. As the density of the leached samples decreases, cation removal increases and resulted in a higher SSA achieved.

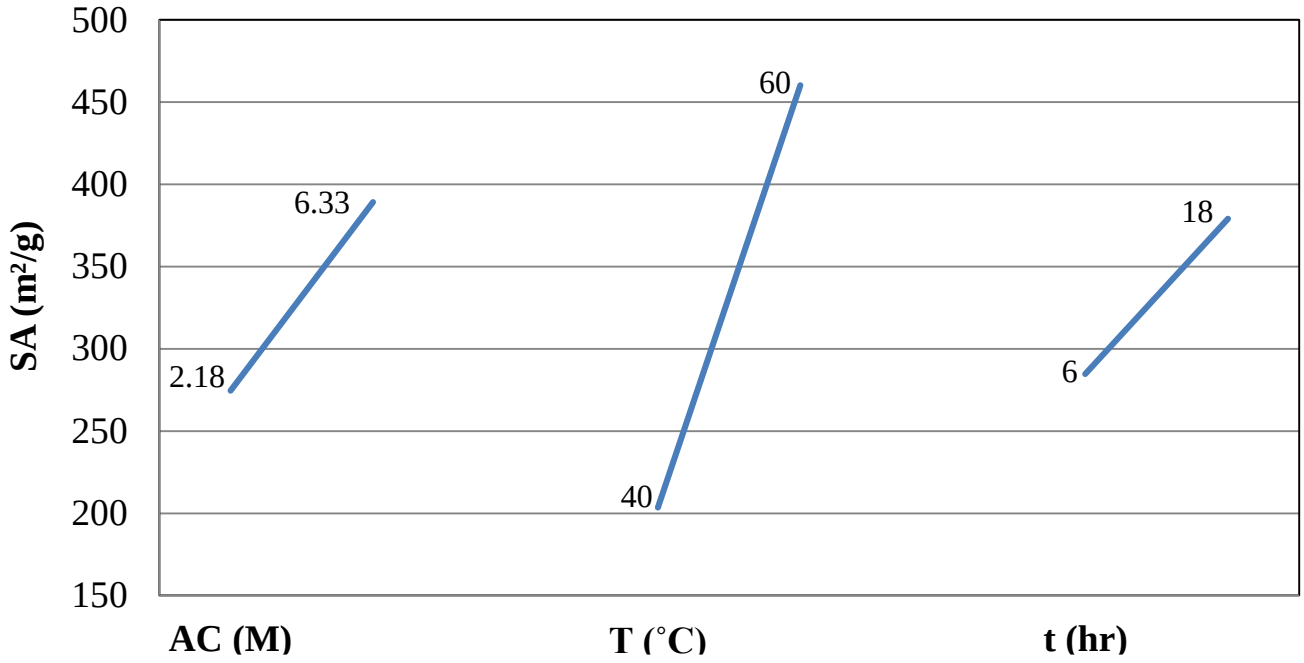

Figure 11: Main Effects of Nitric Acid leached phlogopite with increasing trends in acid concentration, temperature and time.

The main effects of the individual leaching conditions are shown in Figure 11. Acid concentration, leaching time and leaching temperature all indicate main effects with positive gradients, suggest at the higher leaching condition values higher surface area values are obtained. Phlogopite was leached with nitric acid at the high levels of each leaching parameter in N8 from Table 7. Experiment N8 yielded the 3rd highest SSA value instead of the highest SSA as predicted. The silica structure has a high porosity, as a result the SSA measured with the BET has an average variation in measured results of 5% contributing to the comparison of similar values rather difficult. With the SSA results variation taken into consideration, N8 provided a sufficiently large SSA value as predicted. The main effect patterns coincide with the literature as summarized in Section 2.10. The difference in predicted and achieved N8 values also suggests there are possible parameter interactions that affect the SSA of the silica.

A combination of the main effects are plotted against each other and if the effect lines intersect there is a possibility of interaction between the 2 parameters and the angle of intersection indicate the strength of the interaction. The main effects are determined by selecting 2 of the leaching parameters and calculating

the average SSA obtained at each of the possible parameter combinations. The average SSA is calculated for the following combinations:

1. Parameter 1 high level versus parameter 2 low level
2. Parameter 1 high level versus parameter 2 high level
3. Parameter 1 low level versus parameter 2 low level
4. Parameter 1 low level versus parameter 2 high level

The average SSA of the combinations are determined and the possible interactions are shown in Figure 12.

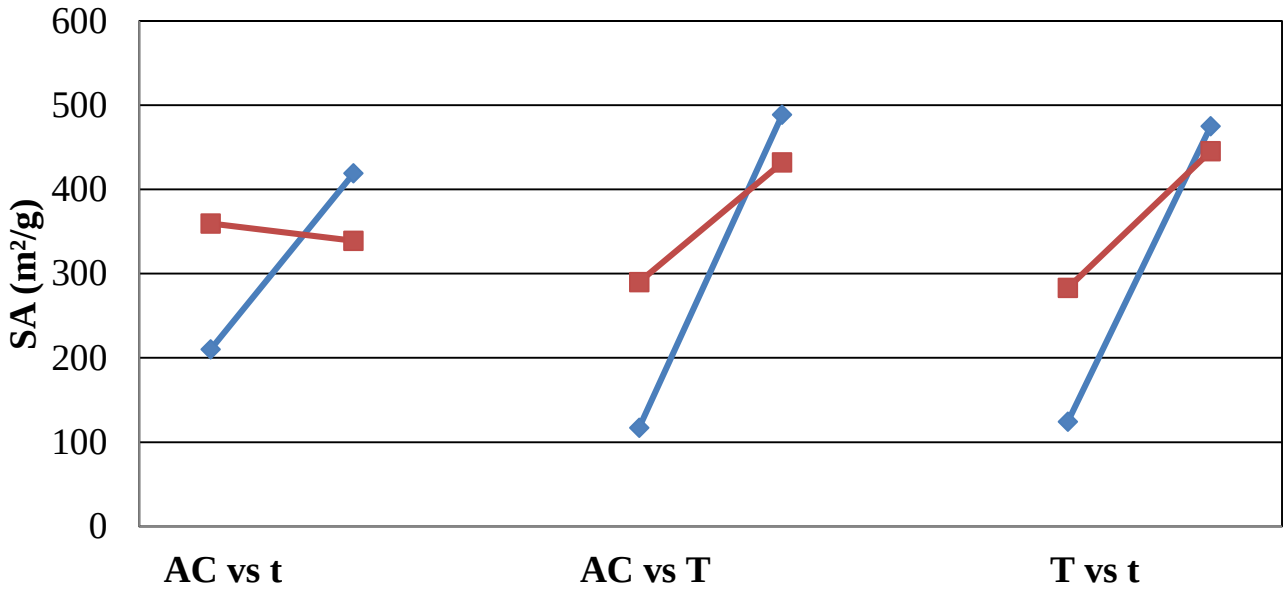

Figure 12: Possible leaching parameter interactions for Nitric Acid leached phlogopite.

The acid concentration (AC) versus time (t) effect lines intersect at a large angle suggesting a large possible interaction on the surface area, suggesting as the AC increases the t has to be decreased. The acid concentration (AC) versus temperature (T) as well as the time versus temperature graphs indicates a smaller interaction effect on the surface area. The phlogopite samples leached with nitric acid were analyzed with XRF as shown in Table 9.

Table 9: XRF results of Nitric Acid leached Phlogopite

%	N1	N2	N3	N4	N5	N6	N7	N8
SiO_2	43.30	50.60	71.00	79.80	49.50	79.20	90.20	90.80
MgO	24.40	20.00	9.10	4.51	21.50	5.65	<0.01	<0.01
Al_2O_3	10.10	8.38	3.66	1.75	7.77	2.23	<0.01	<0.01
Fe_2O_3	7.19	5.88	3.18	1.77	6.16	1.88	0.25	0.17
K_2O	6.89	5.43	3.00	1.67	5.22	1.62	<0.01	<0.01
TiO_2	0.87	1.02	1.10	1.10	0.98	0.56	0.41	0.48
M^+ Rec	2.81	19.98	60.61	78.77	18.18	76.53	98.71	98.72

The XRF results compared to the metal recovery results of Harkonen & Keiski (1984), Table 8, show similar results. Harkonen & Keiski (1984) accomplished a 99.50% cation removal compared to the 98.72% cation removal from Table 9. The leaching results show the larger the surface area, the purer the silica backbone and the greater the cation removal.

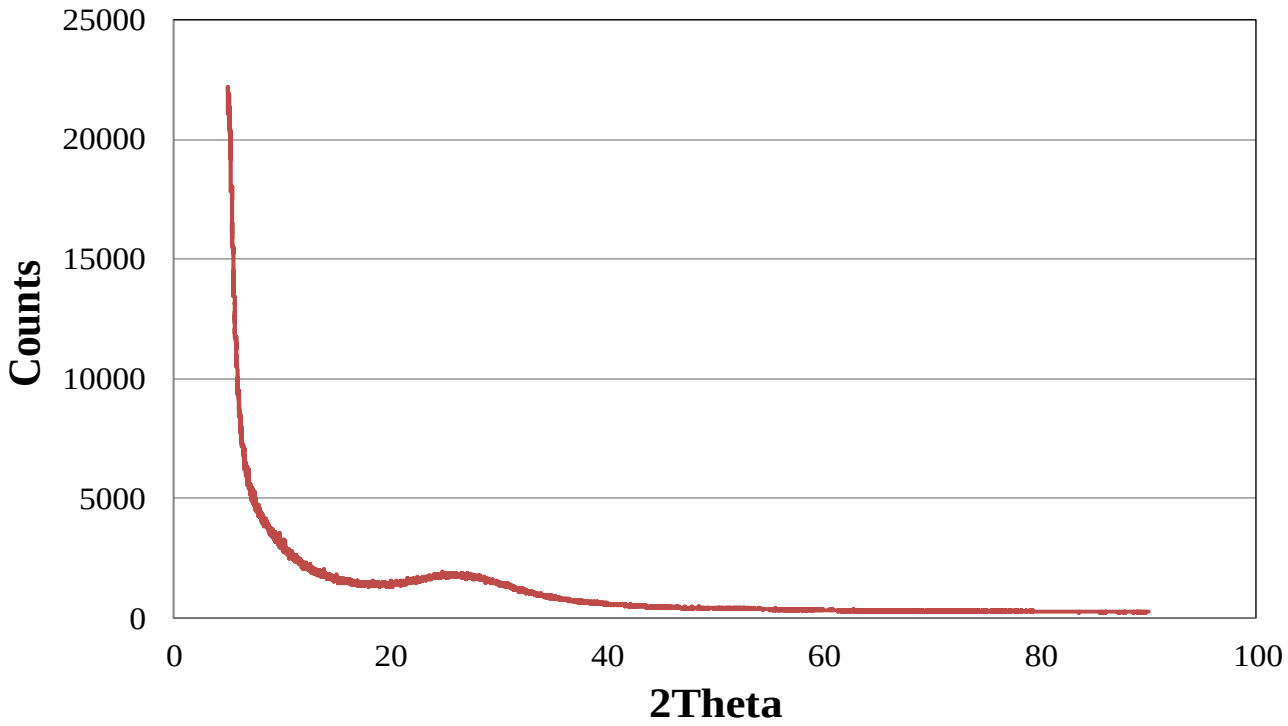

Figure 13: XRD result of N7 showing an amorphous structure obtained after leaching

The XRD results of N7 is shown in Figure 13. The XRD analysis confirms the amorphous structure as reported in literature. During acid leaching the layered

silicates sheets distort, tilting bonds producing apical silanol groups. This distortion results in the long range order of the structure to be lost resulting in an amorphous structure. Wypych *et al* (2004) found that leached phlogopite samples have higher concentrations of species with absent hydroxyl groups (Q_4 species) than species with 1 or 2 hydroxyl groups (Q_3 or Q_2). The increase in Q_4 species concentration is attributed to the substitution of the Al^{3+} in the tetrahedral layers. The leached sample retains the original layered structure indicating no solubilization of the silica backbone was involved in the acid leaching process.

The morphology of the leached sample is shown in Figure 14. The leached samples show clear damage to the edges of the particle, possibly from the edge attack mechanism of the acid as suggested by Kaviratna & Pinnavaia (1994) and Harkonen & Keiski (1984)

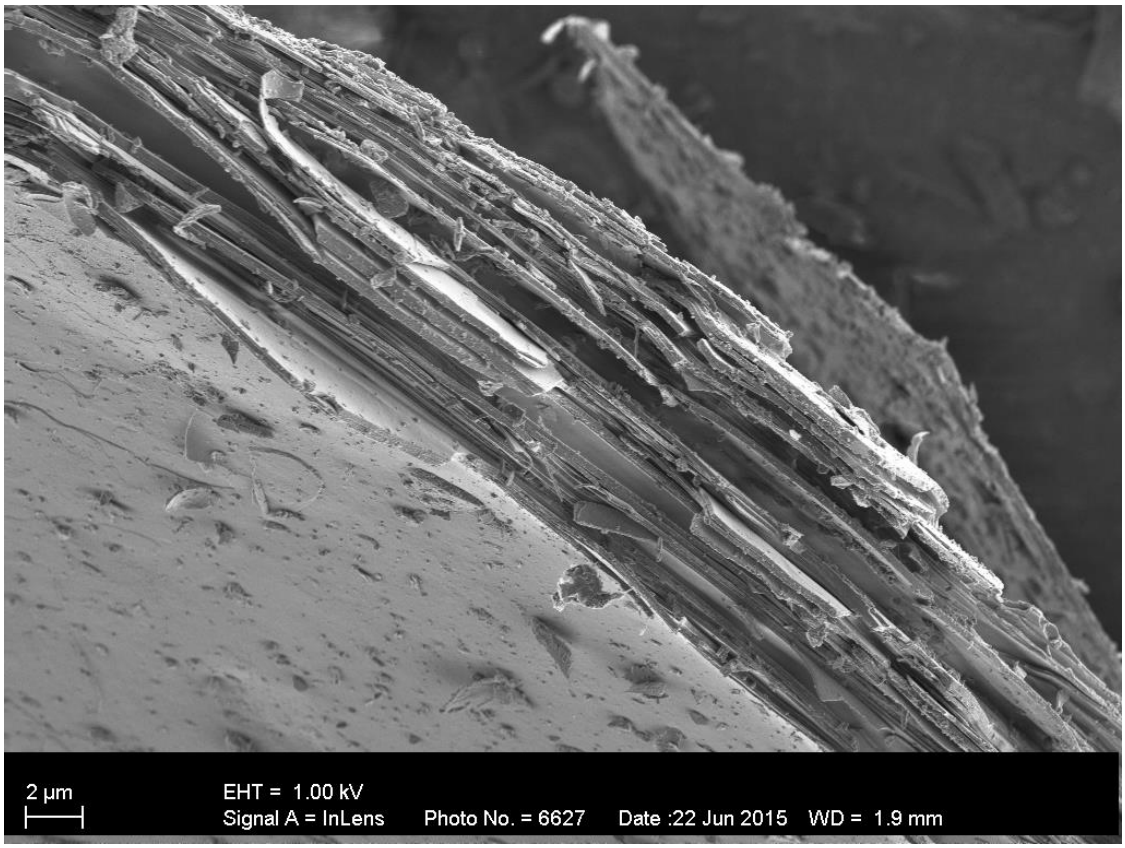

Figure 14: FEG SEM image of N7 of Nitric Acid with clearly damaged edges.

5.3 Hydrochloric Acid

The full factorial experimental design for HCl is shown in Table 10. As discussed in section 4.2, the same leaching conditions are used for nitric acid and hydrochloric acid leaching of phlogopite. The same leaching conditions are used for HNO_3 and HCl to determine the leaching results at both the NR extremes (0 and 1).

Table 10: Full Factorial Experimental Design for Hydrochloric Acid

Number	**AC (M)**	**t (hrs)**	**T (˚C)**	**SA (m^2/g)**	**MR (g/g)**	**ρ (g/cm^3)**
H1	2.18	6	40	29	86.55	2.63
H2	2.18	18	40	131	65.00	2.39
H3	2.18	6	60	311	63.95	2.24
H4	2.18	18	60	326	59.35	2.17
H5	6.33	6	40	116	76.50	2.52
H6	6.33	18	40	258	53.60	2.30
H7	6.33	6	60	320	53.55	2.24
H8	6.33	18	60	302	46.10	2.25

For phlogopite leached with HCl, 2 of the highest specific surface area values obtained are 326 m^2/g and 320 m^2/g from H4 and H7 respectively. Experiment H4 and H7 were both performed at 60 ˚C while H4 was performed at a lower acid concentration and longer leaching time than H7 and this indicates a possible highly significant interaction between acid concentration and time. Harkonen & Keiski (1984) reported an HCl leached phlogopite experiment that achieved a specific surface area of 198 m^2/g, with 9.45 M HCl for 6 hrs at 100 ˚C. The experiment with closest conditions to Harkonen & Keiski (1984) is H7. Harkonen & Keiski (1984) obtained a lower surface area at a higher acid concentration and leaching temperature, indicating the acid concentration and temperature combination as too excessive resulting in a damaged silica structure.

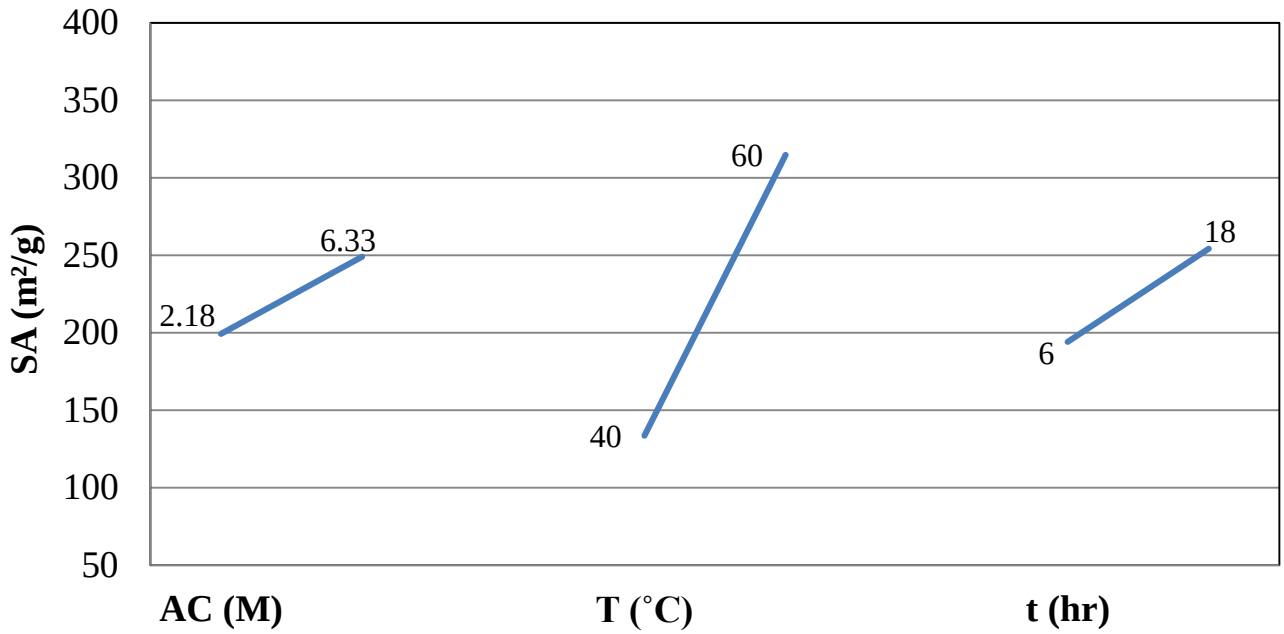

Figure 15: Main effects for leaching conditions for Hydrochloric Acid leached phlogopite with increasing trend of acid concentration, temperature and time

The main effects of the FFED results are shown in Figure 15. These results indicate that all 3 parameters at the higher leaching parameter would results in the higher SSA and show the same trend as Nitric Acid interactions. The phlogopite leached with HCl achieved lower surface area values, higher density values and higher mass recovery values compared to HNO_3. HCl is classified as a strong acid according to its pKa value of -6.3. Compared to HNO_3, HCl has a lower pKa value indicating that it is a stronger acid. However HCl is not an oxidizing agent, resulting in HCl having weaker leaching capability and rendering lower cation removal and lower specific surface area values.

The main effects in Figure 15, suggest the higher levels of the leaching conditions should yield the highest SSA. Experiment H8 was performed at the highest levels of the leaching conditions. Experiment H8 provided the 4th highest SSA silica, the 4 experiments with the highest SA values (H3, H4, H7 and H8) provided similar specific surface area values with the 5% SSA measurement variation taken into account. The variation in expected results of H8 versus the obtained results indicate the parameters interaction affect the SSA.

The possible leaching parameter interactions are shown in Figure 16. The results of leaching phlogopite with HCl indicate possibly significant parameter interaction between acid concentration and time. However for acid concentration versus temperature as well as for time versus temperature, results indicate there may be parameter interactions at the higher leaching conditions levels.

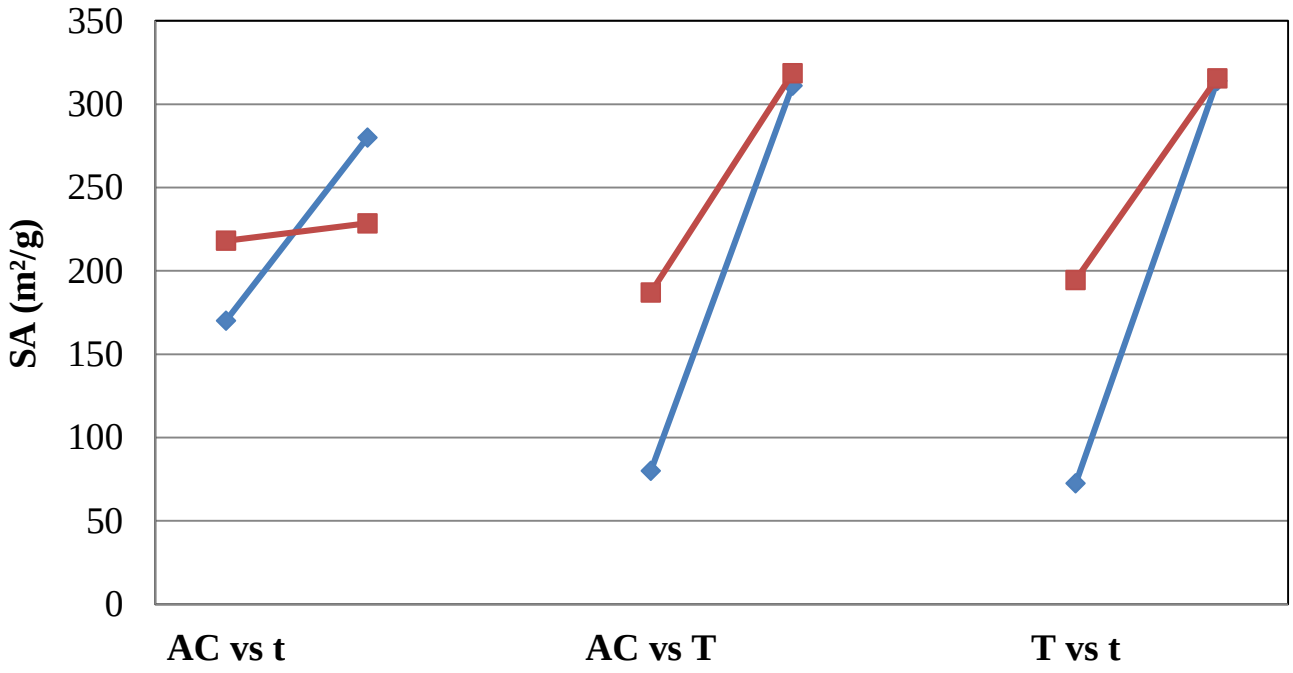

Figure 16: Possible leaching parameter interactions of Hydrochloric Acid leached phlogopite with possible significant interactions of acid concentration and time

The HCl leached phlogopite samples were analyzed with the XRD, the 8 (H1 – H8) samples yielded similar XRD patterns as shown in Figure 17. The XRD analysis reveals HCl leached phlogopite samples retain their crystalline structure. HCl leached phlogopite retaining its crystalline structure suggests little of no solubilization or precipitation of the silica structure took place during leaching (Wypych *et al*, 2004).

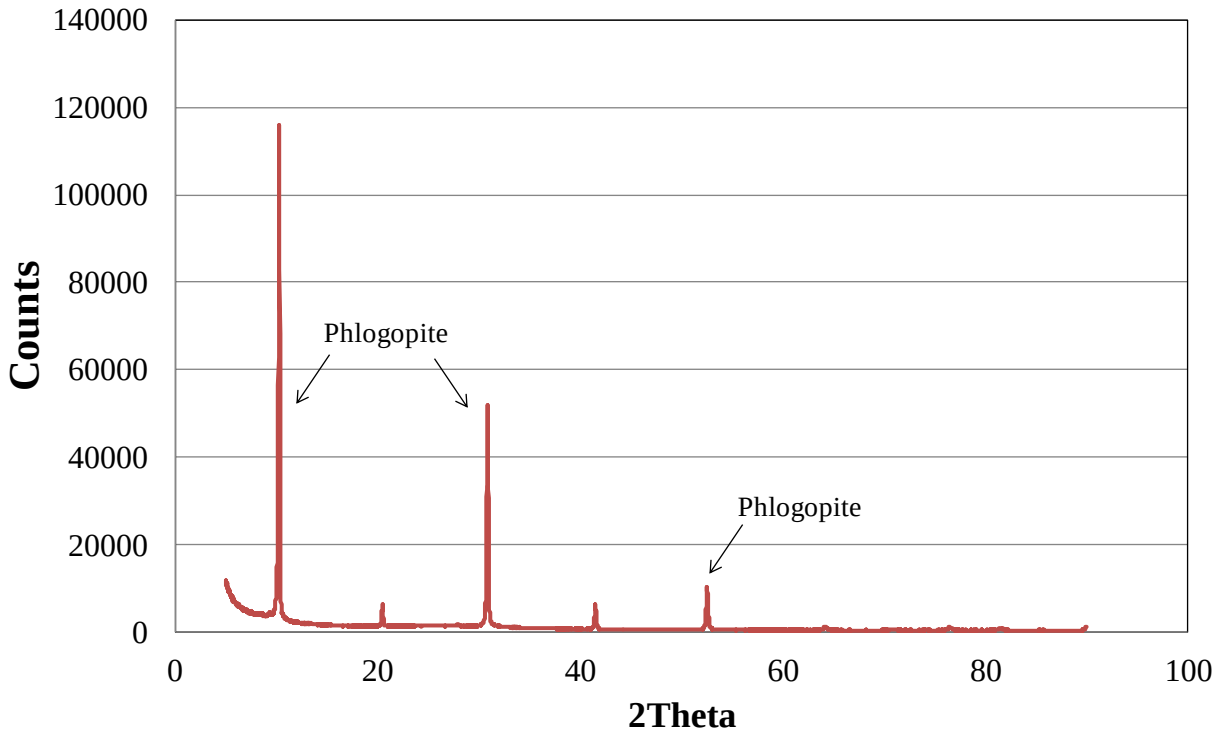

Figure 17: XRD diffraction pattern of phlogopite leached with hydrochloric acid showing the leached structure retaining its original crystalline structure.

5.4 *Aqua Regia*

Phlogopite leached with *aqua regia* exploratory experiments were performed as discussed in Section 4.2. The results were used to design the augmented PFED design with star and center points for improved regression estimation.

5.4.1 *Aqua Regia* Exploratory

The leaching conditions used of HNO_3 and HCl with an additional leaching parameter (NR) were used for *Aqua Regia* Exploratory phlogopite leaching as discussed in Section 3.2. *Aqua Regia* Exploratory, partial factorial experimental design is shown in Table 11.

Table 11: PFED for *Aqua Regia* Exploratory phlogopite leaching

No	**AC (M)**	**NR**	**t (hrs)**	**T (˚C)**	**SA (m^2/g)**	**MR (g/g)**	**ρ (g/cm^3)**
A1	2.18	0.56	6	40	21	87.70	2.62
A2	2.18	0.73	18	40	191	74.70	2.26
A3	2.18	0.73	6	60	396	57.90	2.08
A4	2.18	0.56	18	60	450	52.55	2.07
A5	6.33	0.73	6	40	197	49.65	2.39
A6	6.33	0.56	18	40	432	69.55	1.93
A7	6.33	0.56	6	60	463	43.25	1.98
A8	6.33	0.73	18	60	428	44.70	2.04

Aqua Regia Exploratory conditions rendered silica with a surface area of 463 m^2/g (A7) and 450 m^2/g (A4). The largest specific surface area values were obtained at the high level leaching temperature and lower level leaching NR, suggesting a highly significant parameter dependency on SSA.

The silica structure has a high porosity, as a result the SSA measured with the BET has an average variation in measured results of 5% contributing to the comparison of similar values rather difficult.

The main effects of the individual leaching conditions are shown in Figure 18. The acid concentration, leaching time and temperature results suggest positive gradient main effect trends, similar result trends as seen with HNO_3 and HCl leaching. The nitrate ratio results indicate a negative gradient trend. The main effects suggest the maximum specific surface area is achieved at the high level leaching conditions of acid concentration, leaching time and temperatures and at lower level leaching conditions of nitrate ratio. The main effects indicate in which direction the leaching conditions need to be changed in order to achieve the maximum silica specific surface area.

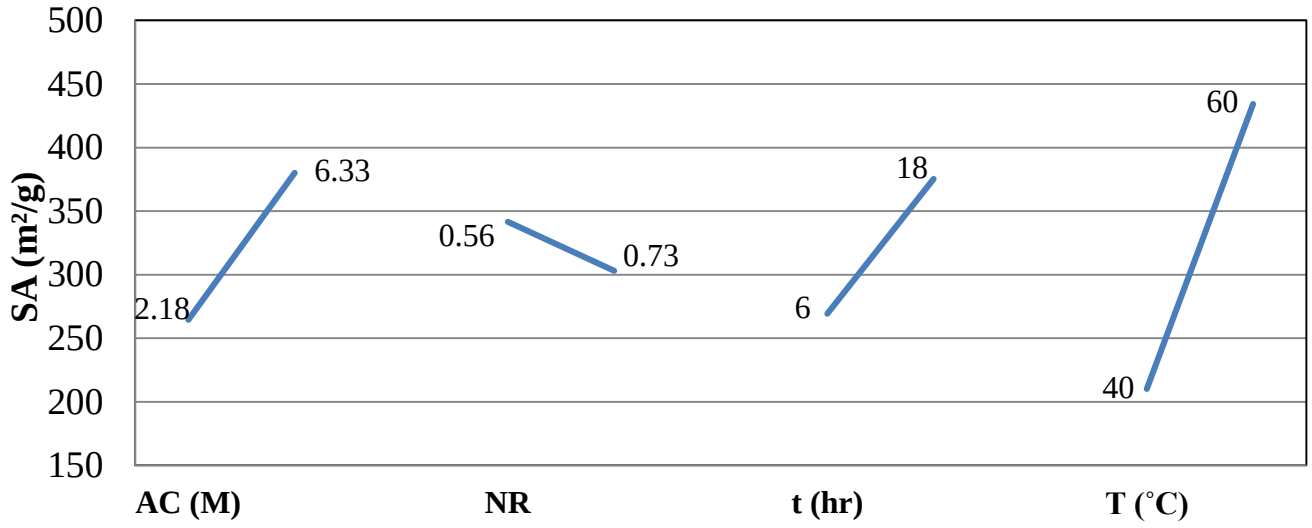

Figure 18: Main Effects of leaching conditions for *Aqua Regia* Exploratory with increasing trends of acid concentration, temperature and time similar to HCl and HNO_3 with decreasing nitrate ratio trend

The PFED SSA results are used to estimate possible parameter interactions, the possible interactions are shown in Figure 19. Similar possible leaching conditions interactions of *Aqua Regia* Exploratory were also seen in HNO_3 and HCl possible interactions. The interaction results suggest a possible strong interaction between acid concentration and leaching temperature, whereas there might not be significant interaction between acid concentration and time and leaching temperature and time.

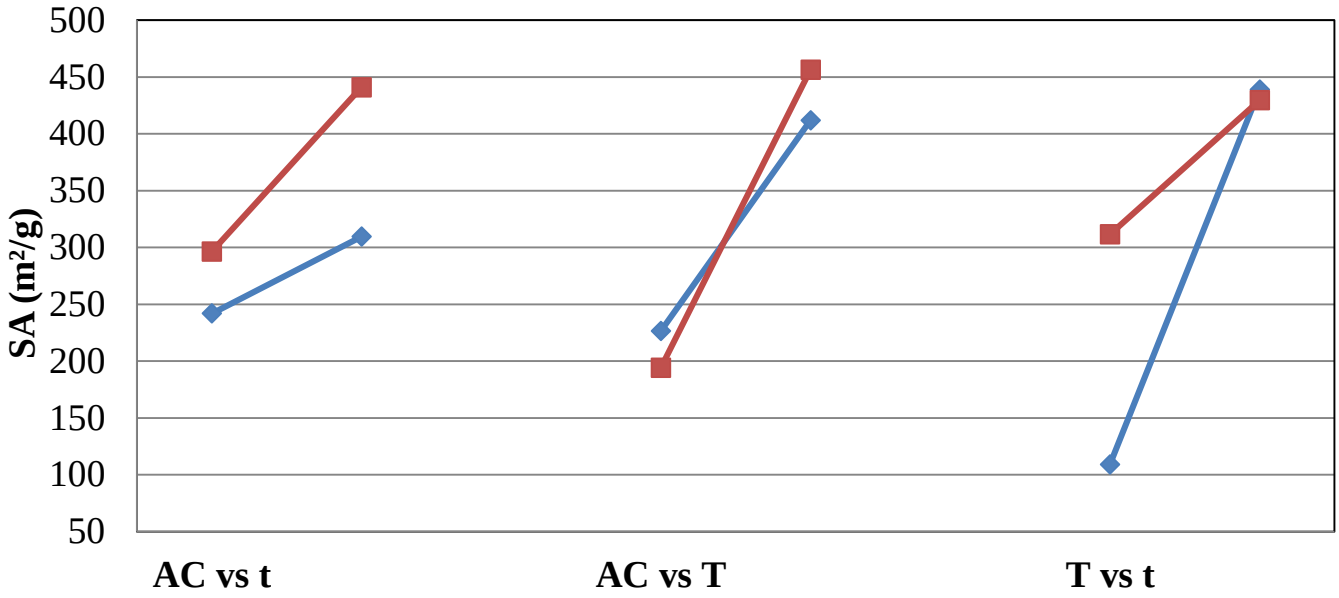

Figure 19: Possible leaching parameter interactions for *Aqua Regia* Exploratory with possible significant interactions between acid concentration and temperature

Phlogopite leached with *Aqua Regia* Exploratory samples were analyzed with XRF to determine changes in composition and overall metal recovery as shown in Table 12.

Table 12: Leached sample compositions from XRF results of *Aqua Regia* Exploratory

%	A1	A2	A3	A4	A5	A6	A7	A8
SiO_2	42.70	52.00	70.20	74.20	52.30	86.80	89.40	89.30
MgO	24.10	19.10	10.20	6.64	19.80	1.41	<0.01	<0.01
Al_2O_3	9.69	7.25	3.71	2.81	7.67	0.23	<0.01	<0.01
Fe_2O_3	7.34	5.61	3.30	2.36	5.28	0.54	0.20	0.13
K_2O	7.38	5.70	2.73	2.55	4.58	0.38	<0.01	<0.01
TiO_2	1.06	1.14	1.05	1.02	0.90	0.35	0.35	0.40
M^+ Rec	2.57	23.74	58.74	69.77	24.86	94.29	98.91	98.96

Phlogopite consists on average of 41.72% SiO_2, the XRF results of A6 – A8, suggest almost pure silica was recovered and the cations (magnesium, aluminum and potassium) were successfully removed. Experiments A6 to A8 provided lower silica surface area values compared to surface area values

obtained from HNO_3, however the cation removal achieved by A6 – A8 are highly similar to cation removal achieved by HNO_3. Samples with the highest SSA values (A6 – A8) were analyzed with XRD and provided similar diffraction patterns as shown in Figure 20.

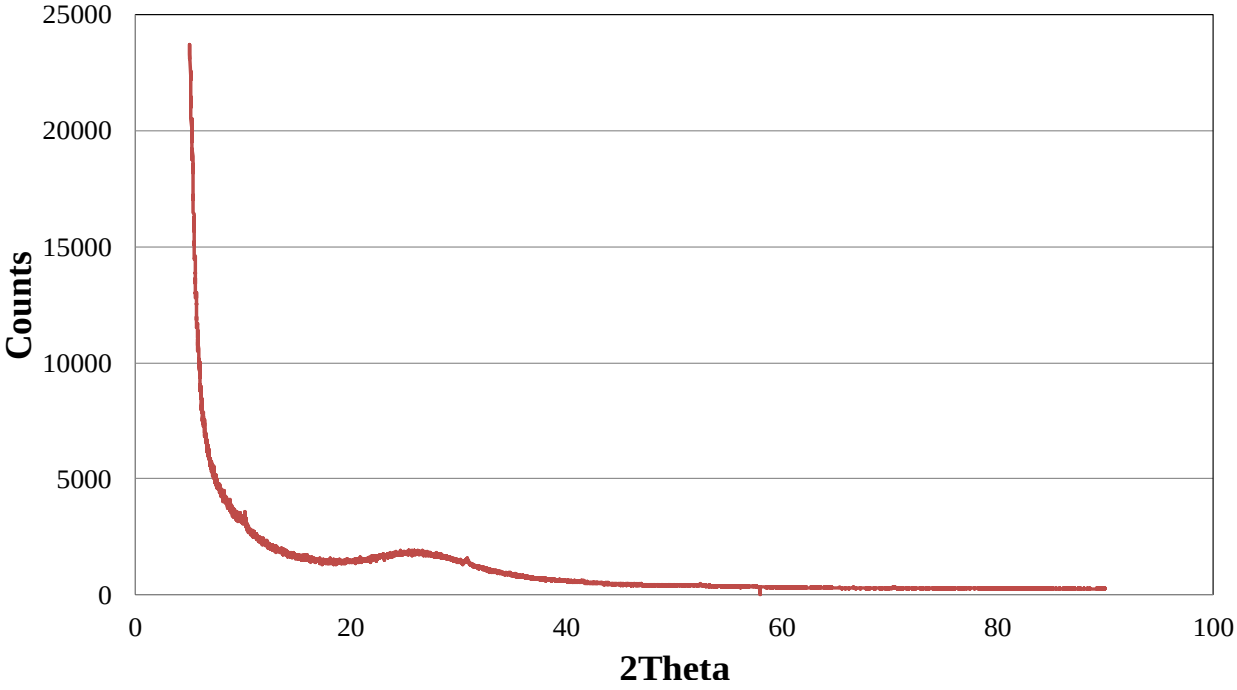

Figure 20: XRD of *Aqua Regia* Exploratory samples (A6 – A8) with amorphous leached structure

The amorphous structure (A6 – A8) corresponds to previous literature. Wypych *et al* (2004) found that when layered silicates are leached under acidic conditions, the bonds distort resulting in an amorphous structure before the structure is reestablished into its original layered structure as seen in Figure 21.

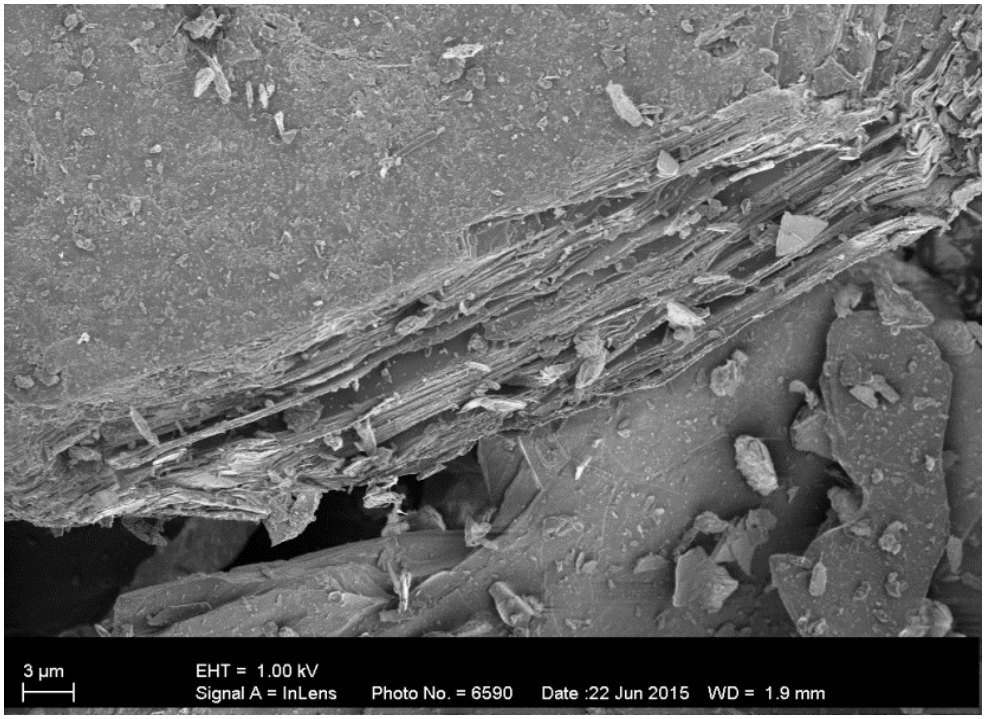

Figure 21: FEG SEM images of leached layered structure

5.4.2 *Aqua Regia* Final

The main effects obtained from the previous experiments; Nitric Acid, Hydrochloric Acid and *Aqua Regia* Exploratory, formed the basis of the partial factorial experimental design of *Aqua Regia* Final. The following main effects were obtained from the previous experiments:

- Acid Concentration: positive gradient trend
- Nitrate ratio: negative gradient trend
- Temperature: positive gradient trend
- Time: positive gradient trend

The results of previous experiments yielded the following Aqua Regia Final experimental design as shown in Table 13.

Table 13: Partial Factorial Experimental Design for *Aqua Regia* Final

No	**AC (M)**	**NR**	**t (hrs)**	**T (˚C)**	**SA (m^2/g)**	**MR (g/g)**	**ρ (g/cm^3)**
B1	4.26	0.47	12	50	408	45.90	2.05
B2	4.26	0.64	24	50	346	46.30	2.13
B3	4.26	0.64	12	70	480	48.35	1.96
B4	4.26	0.47	24	70	343	46.70	2.15
B5	8.40	0.64	12	50	515	46.55	1.97
B6	8.40	0.47	24	50	357	46.05	2.17
B7	8.40	0.47	12	70	314	43.90	2.13
B8	8.40	0.64	24	70	334	38.20	2.09

The 2 highest specific surface area values obtained are 515 m^2g (B5) and 480 m^2/g (B3). Phlogopite leached with *Aqua Regia* experiment B5, provided mesoporous silica with average pore width of 2.62 nm and average pore volume of 0.36 cm^3/g. The silica SSA values of *Aqua Regia* Final are similar to the SSA values obtained by phlogopite leached with Nitric Acid and higher than the values achieved through leaching with Hydrochloric Acid and *Aqua Regia* Exploratory. Phlogopite leached with *Aqua Regia* obtained higher SSA than HNO_3 and HCl. This can be explained by *Aqua Regia* having 3 strong

oxidizing agents, HNO_3, Cl_2 and NOCl. These 3 strong agents, oxidize the cations to higher oxidation states increasing their affinity to react with the highly negative nitrate and chloride ions available. This gives Aqua Regia its unique ability of providing higher silica SSA values at lower acid concentrations.

The silica structure has a high porosity, as a result the SSA measured with the BET has an average variation in measured results of 5% contributing to the comparison of similar values rather difficult.

The highest SSA values achieved from A*qua Regia* Final experiments were obtained at different acid concentration and leaching temperatures suggesting a significant parameter dependency of AC and T on SSA values. However, higher SSA values were obtained at the same nitrate ratio and leaching time.

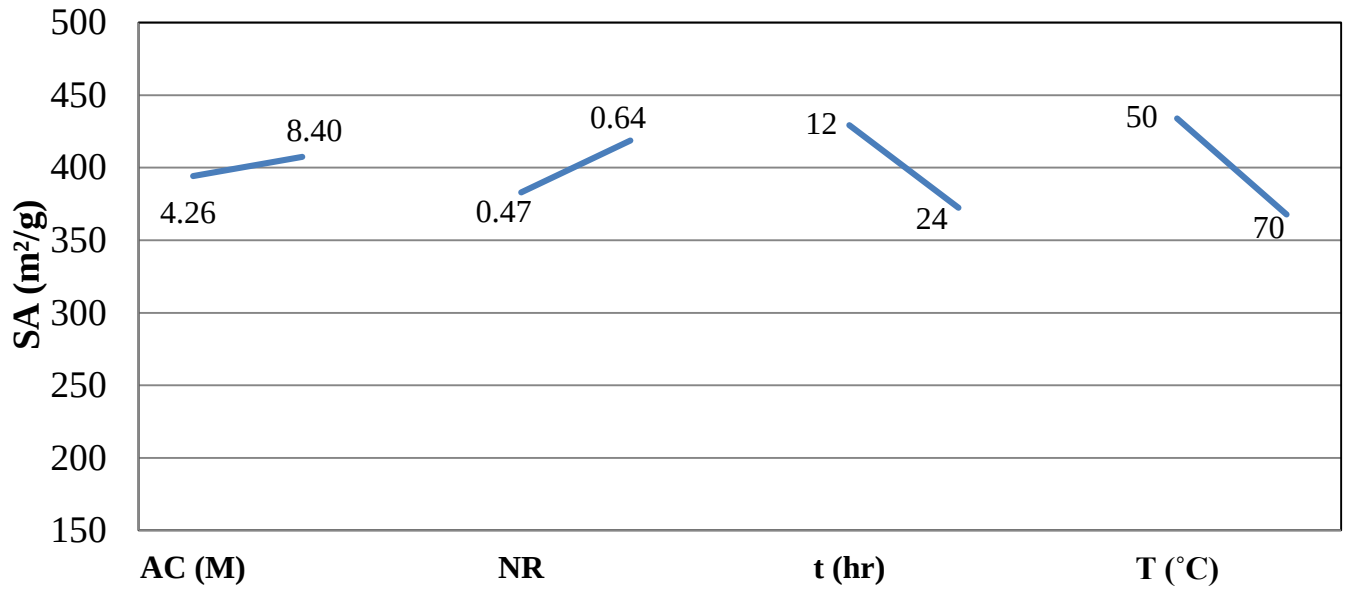

Figure 22: Main Effects of *Aqua Regia* Final increasing trends of acid concentration and nitrate ratio and decreasing trends of time and temperature

The main effects of the individual leaching parameters shown in Figure 22, suggest experiments performed at the higher level of acid concentration and nitrate ratio and at the lower level of leaching time and temperature will provide the highest silica SSA values. Therefore the experiment performed at 8.40 M,

NR of 0.64, 12 hours at 50 ˚C, should provide the highest SSA. Experiment B5 was performed at these conditions and provided the highest SSA of 515 m²/g.

Possible parameter interactions for *Aqua Regia* Final are shown in Figure 23. Similar to the previous set of experiments possible interactions, the acid concentration versus time relationship suggest there may not be a significant parameter interaction within the leaching conditions range. The acid concentration versus temperature results indicates no parameter interaction. The time versus temperature suggest a highly significant possible interaction, similar to the results obtained from Nitric Acid. The experimental results suggests as the leaching time increases the temperature has to decrease.

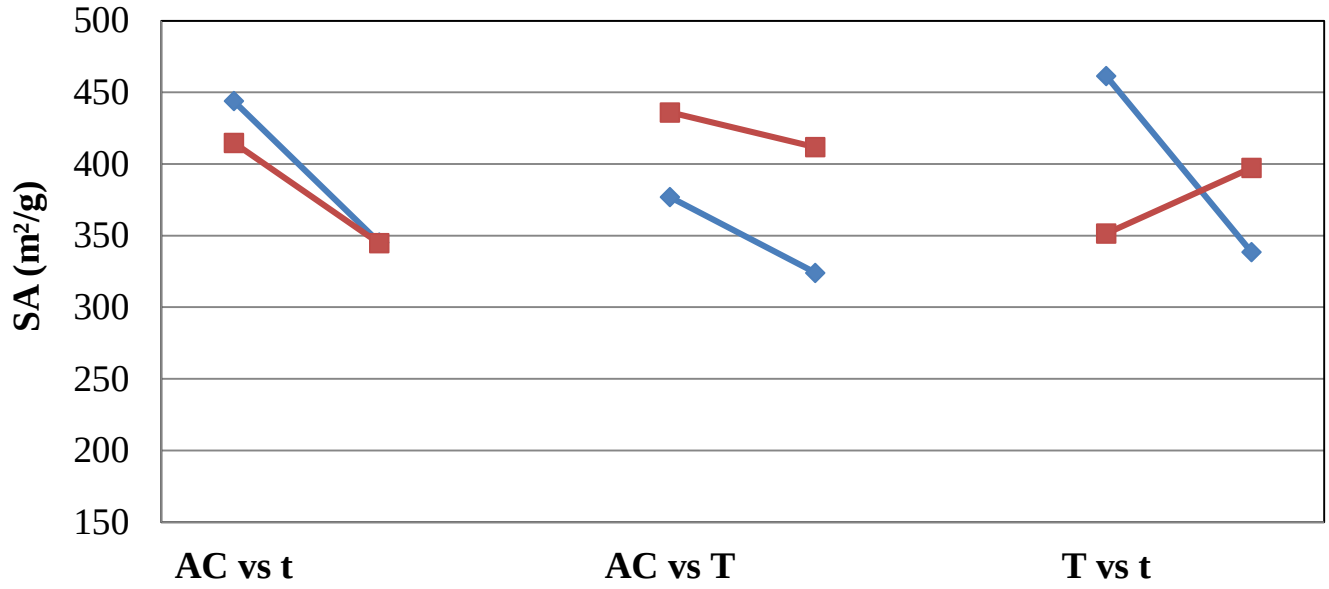

Figure 23: Possible leaching interactions for *Aqua Regia* Final leached phlogopite with possibly significant interaction between temperature and time

The main effects of the results of *Aqua Regia* Final experiments differ from the main effects of *Aqua Regia* Exploratory as shown in Table 14.

Table 14: Difference in gradient trends for *Aqua Regia* Exploratory and Final

Main Effect	***Aqua Regia* Exploratory**	***Aqua Regia* Final**
Acid Concentration	Positive	Positive
Nitrate Ratio	Negative	Positive
Time	Positive	Negative
Temperature	Positive	Negative

The differences in the main effects of *Aqua Regia* Exploratory and Final, suggests the maximum silica specific surface area achievable, is possible located within the 2 ranges. *Aqua Regia* Final was augmented with center points and star points as discussed in Section 4.2 and is shown in Table 15.

Table 15: Centre Points and Star Point Experiments for *Aqua Regia* Final

	No	**AC (M)**	**NR**	**t (hrs)**	**T (˚C)**	**SA (m^2/g)**	**MR (g/g)**	**ρ (g/cm^3)**
Centre Points	B9	6.33	0.56	18	60	405	48.95	2.08
	B10	6.33	0.56	18	60	411	49.75	2.04
Star Points	B11	3.41	0.56	18	60	367	49.05	1.96
	B12	9.23	0.56	18	60	401	51.75	1.93
	B13	6.33	0.44	18	60	380	44.30	2.04
	B14	6.33	0.68	18	60	407	43.70	2.05
	B15	6.33	0.56	9.6	60	395	44.20	2.02
	B16	6.33	0.56	26.4	60	388	42.45	2.01
	B17	6.33	0.56	18	46	393	39.70	2.02
	B18	6.33	0.56	18	74	335	44.60	1.99

Star points and center points of the PFED were performed to investigate the non-linearity of the regression model predicting surface area from the leaching conditions. The main effects of the PFED results, the center point and star points results are shown in Figure 24.

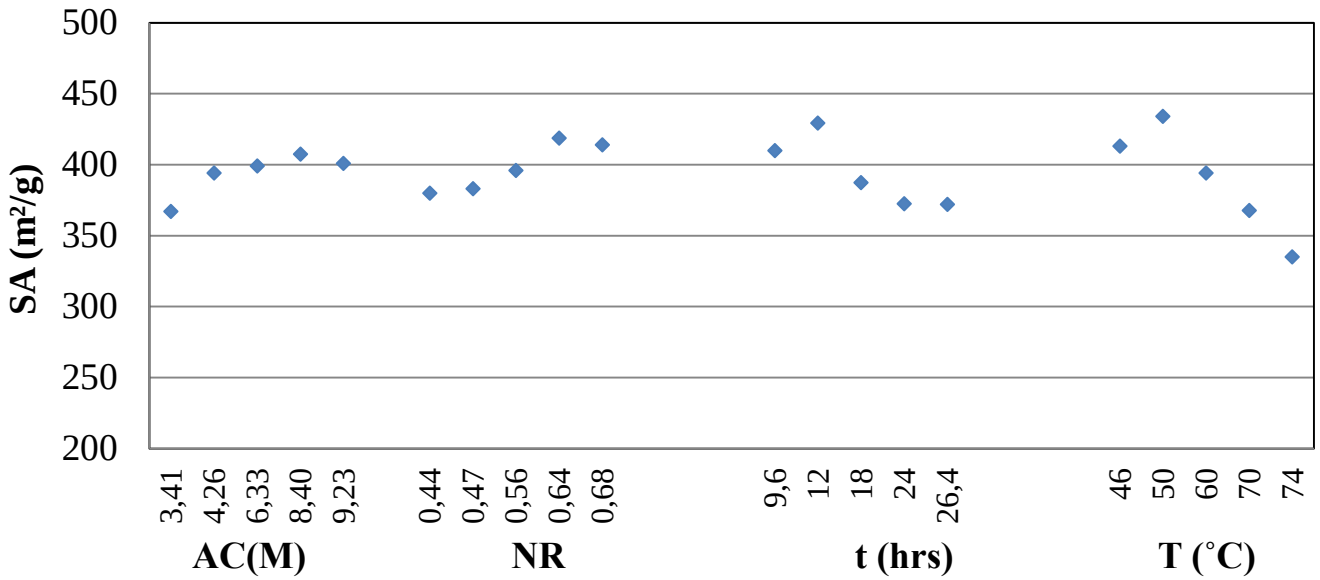

Figure 24: Main effects for *Aqua Regia* Final with PFED, star and center point results

The acid concentration main effect trend suggest as the acid concentration increases the average specific surface area increases. The trend indicates the maximum surface area obtained is at 8.40 M, however similar average surface areas values were achieved at acid concentration between 4.26 M and 8.40 M. At concentrations values higher than 8.40 M the acid concentration is too high resulting in significant damage to the silicon backbone. This general trend conforms to literature (Section 2.10). The nitrate main effect indicates as the nitrate ratio increases (more nitric acid than hydrochloric acid in *aqua regia*), the surface area increases. The average maximum specific surface area is achieved at nitrate ratio of 0.64 where after the surface area decreases slightly.

The main effect of leaching time, suggests the specific surface area increases mutually as the leaching time increases but decreases after an optimal leaching temperature of 12 hrs has been reached is clearly indicated. This supports literature (Section 2.9) if the leaching time is extensive the silica structure is selectively leached significantly damaging the structure. The main effects of leaching temperature results indicate an increase in surface area until an optimal leaching point is reached followed by a sharp decrease in surface area. On average the maximum surface area is achieved at 50 ˚C. Below the optimal temperature of 50 ˚C, the temperature is to low resulting in a slower reaction

rate, and above the optimal, significant damage is caused to the silicon backbone.

The leached samples which provided the highest SSA values (B3 & B5) were sent for XRD analysis and provided similar amorphous spectrum as shown in Figure 25. The samples analyzed with XRD was inspected with FEG SEM as shown in Figure 26. The FEG SEM image verifies the leached samples retained their original layered platelet morphology was found by Wypyth *et al* (2004). Wypyth *et al* (2004) confirmed under acidic leaching conditions the amorphous structure is reestablished forming a crystalline structure. This observations confirms higher Q_4 (hydroxide absent) species were formed on the silica surface during leaching and lower concentration Q_2 and Q_3 species were formed. These conditions confirm no precipitation or solubilization of the silica structure took place during leaching.

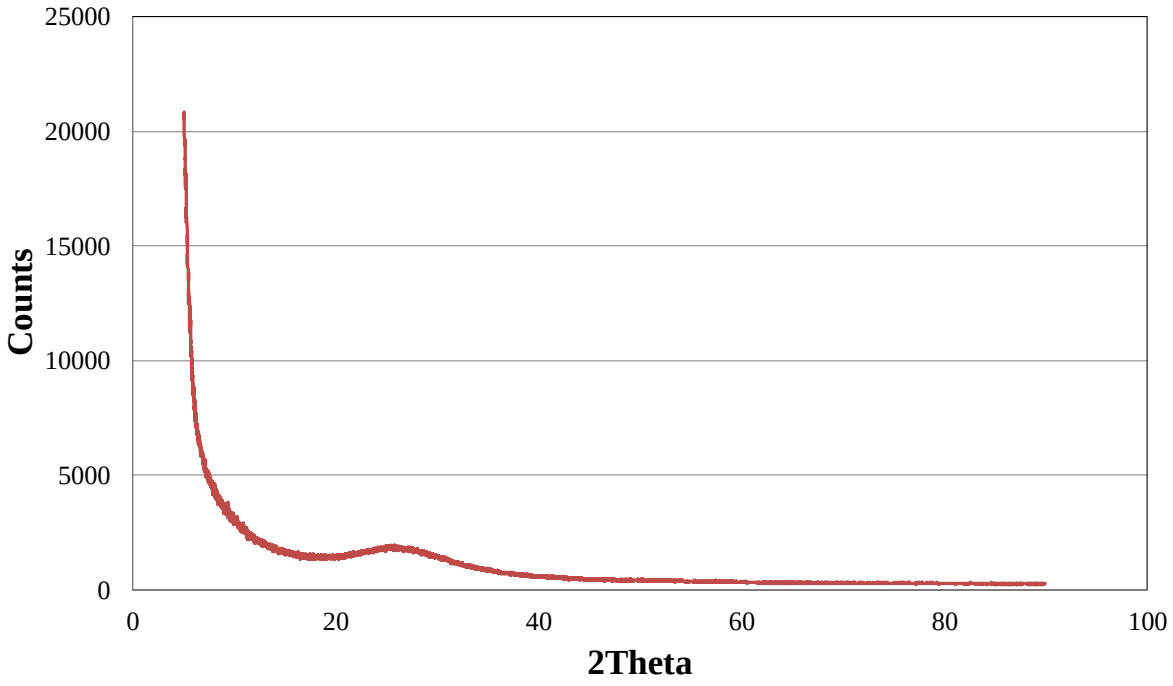

Figure 25: XRD analysis of B5 of *Aqua Regia* Final showing an amorphous leached structure

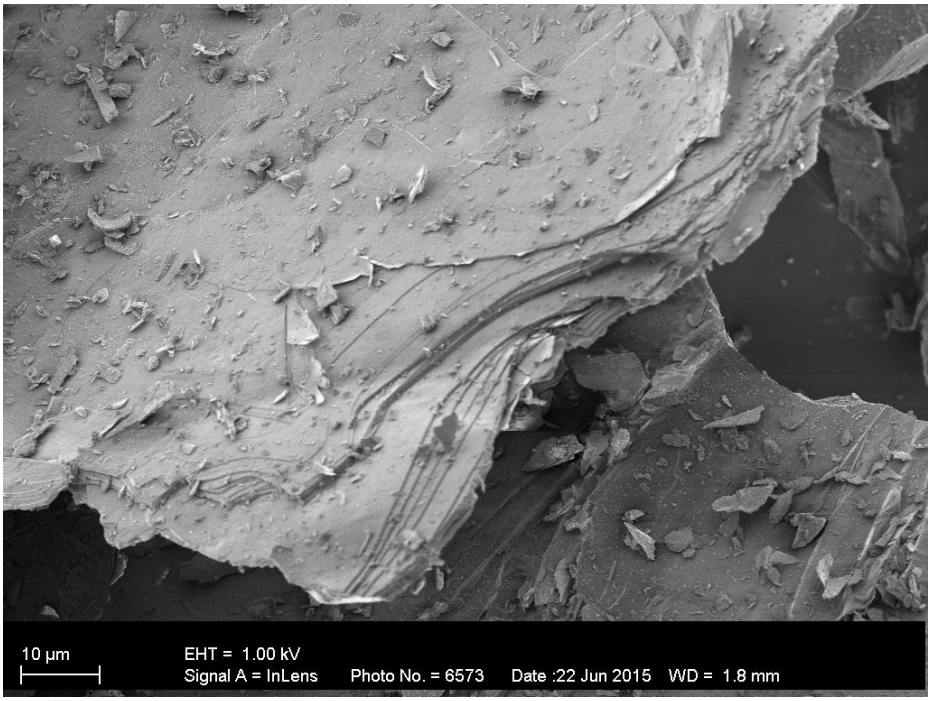

Figure 26: FEG SEM images of B5 of *Aqua Regia* Final

The phlogopite leached in the PFED with *Aqua Regia* in Final, was analyzed with the XRF and the results are shown in Table 16.

Table 16: Composition of phlogopite leached with *Aqua Regia* Final XRF analysis

%	B1	B2	B3	B4	B5	B6	B7	B8
SiO_2	84.80	88.60	87.50	80.90	88.90	82.10	85.00	87.70
MgO	1.88	<0.01	<0.01	1.89	<0.01	1.88	1.77	0.28
Al_2O_3	0.04	<0.01	<0.01	<0.01	<0.01	0.26	<0.01	0.10
Fe_2O_3	0.79	0.24	0.16	0.81	0.13	0.70	0.64	0.18
K_2O	<0.01	<0.01	<0.01	<0.01	<0.01	0.12	<0.01	<0.01
TiO_2	0.16	0.36	0.14	1.58	0.18	0.95	0.21	0.44
M^+ Rec	94.35	98.81	99.41	91.58	99.39	92.33	94.86	98.03

Experiments B5 and B3 provided the highest surface area values of 515 m^2g and 480 m^2/g (Table 13) as well as the highest cation recovery from the phlogopite structure. Experiment B5 removed 99.39% of the cations from the structure and B3 removed 99.41%. The cation removal achieved through phlogopite leaching

with *Aqua Regia* is approximately identical to the cation removal achieved by Harkonen and Kieski (1984) as shown in Table 8.

5.5 Combined Results

The results for Nitric acid, Hydrochloric Acid and *Aqua Regia* Exploratory and Final were combined. The combined results are used to perform a stepwise regression in which the silica specific surface area can be estimated from the acid concentration, nitrate ratio, leaching time and temperature. The regression statistics and ANOVA are shown in Table 17.

Table 17: Regression statistics and ANOVA results of combined results

Regression Statistics	
Multiple R	0.95
R^2	0.90
Adjusted R^2	0.88

	Coefficients	***Standard Error***	***P-value***	***Lower 95%***	***Upper 95%***
Intercept	-1895.10	196.37	2.87×10^{-11}	-2294.18	-1496.03
T^2	-0.27	0.08	2×10^{-3}	-0.43	-0.10
AC * T	-1.93	0.33	1.18×10^{-6}	-2.60	-1.27
T * t	-0.61	0.11	5.24×10^{-6}	-0.84	-0.38
AC	119.94	17.97	1.15×10^{-7}	83.43	156.46
T	53.05	7.71	6.39×10^{-8}	37.37	68.72
t	36.52	6.21	1.23×10^{-6}	23.90	49.15
NR	109.95	21.42	1.15×10^{-6}	66.42	153.49

From the statistical analysis the regression with a $R^2 = 0.90$ is determined as shown in Equation 16

$$SSA = -0.27 * T^2 - 1.93 * AC * T - 0.61 * T * t + 119.94 * AC + 53.05 * T + 36.52 * t + 109.95 * NR - 1896.10 \quad (16)$$

where SSA is the estimated silica specific surface area in m²/g, AC the acid concentration in M, T the leaching temperature in ˚C, t the leaching time in hours and NR the nitrate ratio.

Confirmation experiments were performed to confirm the accuracy of the regression. Along with the confirmation experiments, Harkonen and Keiski (1984) leaching conditions were tested with the regression as shown in Table 18.

Table 18: Confirmation experiments and Harkonen and Keiski (1984) experiments results for comparison

No	**AC (M)**	**NR**	**t (hrs)**	**T (˚C)**	**Actual SSA (m²/g)**	**Predicted SSA (m²/g)**	**Difference %**
B19	7.16	0.64	12	50	439	399	9
B20	4.25	0.64	12	64	483	430	11
B21	4.25	0.64	12	36	117	128	9
B22	4.26	0.64	24	70	356	364	2
B23	8.40	0.47	24	70	297	282	5
B24	4.26	0.47	12	70	458	422	8
B25	8.40	0.64	12	70	338	376	11
Harkonen	5.71	1	0.17	100	508	430	15
Harkonen	5.71	1	5	100	396	311	21

The confirmation experiments were performed and estimated with the regression, the results are shown in Figure 27.

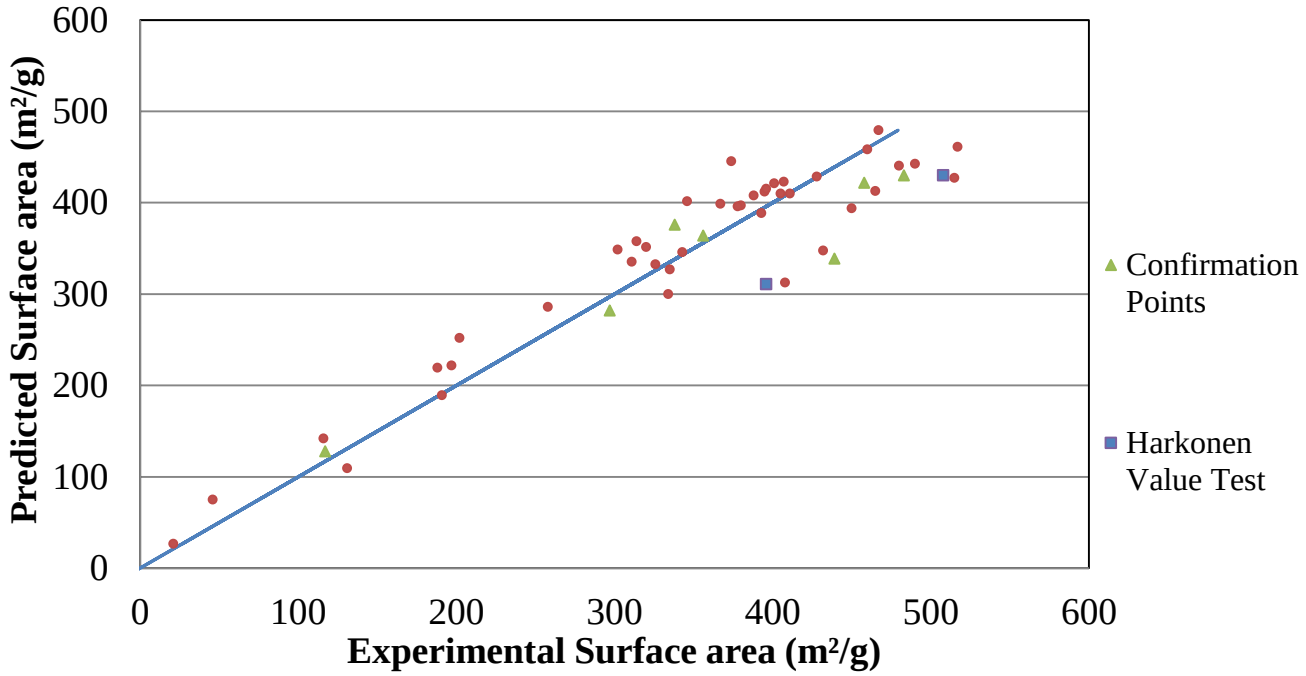

Figure 27: Confirmation experiments results and Harkonen and Keiski (1984) results versus surface area results obtained

The confirmation experiments specific surface area values closely resemble the surface area values of the experimental and predicted values, reinforcing the reliability and accuracy of the regression. The individual leaching conditions main effect is shown in Figure 28 and discussed separately.

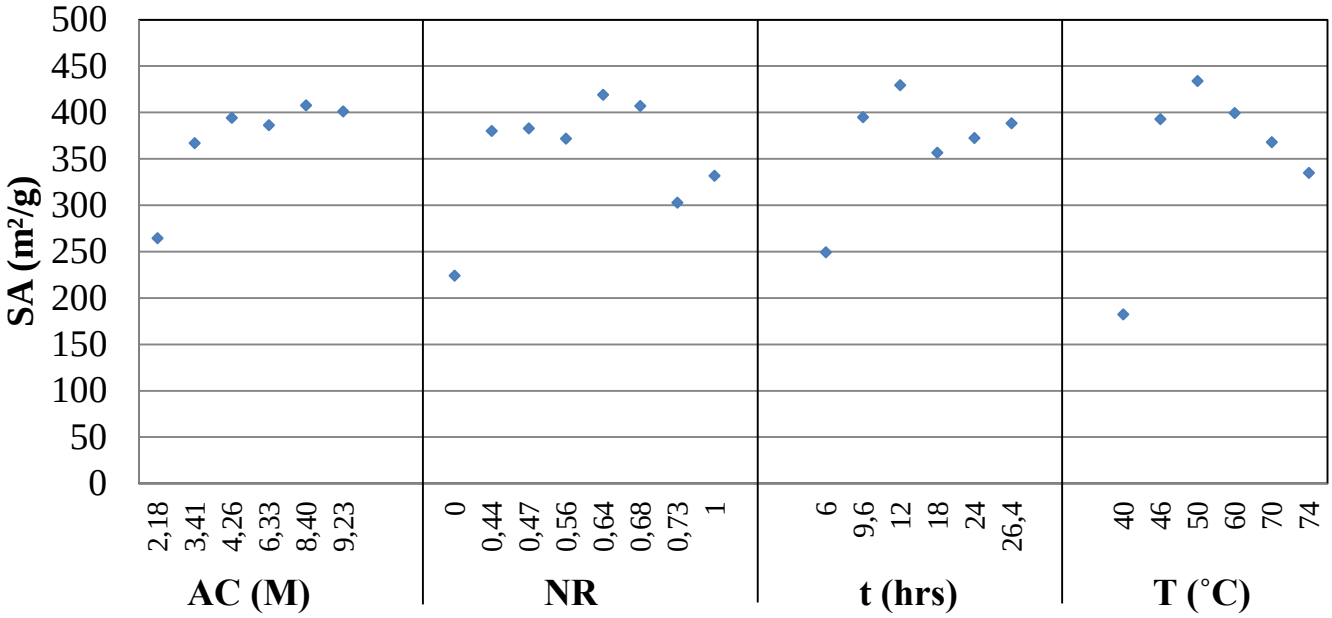

Figure 28: Phlogopite leaching SSA results of the combined results of Nitric Acid, Hydrochloric Acid and *Aqua Regia*

- **Acid Concentration**

The main effects of acid concentration based on average values, suggest an increasing trend of surface area with increasing acid concentration, the increasing trend is verified with the regression coefficient. On average the maximum silica specific surface area values are obtained in the acid concentration range of 4.26 – 8.40 M. At acid concentrations higher than 9.23 M the specific surface area of the silica decreases slightly. The surface area decreases due to Si^{4+} ion being removed from the tetrahedral layer, as suggested by literature (Section 2.5), where the potassium is first selectively leached from the interlayer, followed by the cations from the octahedral layer and lastly the silicon ions from the tetrahedral layer.

- **Nitrate ratio**

The main effects of the average values of the nitrate ratio, indicate hydrochloric acid provides a lower specific surface area followed by nitric acid and then *aqua regia*. As the nitrate ratio increases the surface area increases, however, the maximum surface areas is achieved at nitrate ratio of 0.64 (*Aqua Regia* Final), at nitrate ratios higher than 0.64 the average surface area values decrease.

- **Leaching time**

The main effect for leaching time suggests an interesting trend. As the leaching time increases the specific surface area of the silica increases up till 12 hrs, there after the average surface area decreases. Closer inspection of leaching conditions reveal, at longer leaching periods higher surface area values were obtained at lower temperatures, suggesting a strong interaction between leaching time and temperature. Similar surface area values to Harkonen & Keiski (1984) were obtained at shorter leaching periods by increasing the leaching temperatures, implying a strong leaching time and temperature dependency. Literature support the premise of an extended leaching interval increases the surface area of the silica, however if the leaching period is too long the selective leaching of metals is replaced by selective removal of silicon (Section 2.6). The time versus temperature interaction is verified with the regression and proves to provide a statistically significant parameter dependency on SSA.

- **Leaching Temperature**

The main effects suggest an increasing SSA trend with increasing leaching temperature. This increasing trend follows a parabolic curve as confirmed with the statistically significant regression coefficients. From the main effects of the combine results for leaching temperature, the maximum silica SSA values are obtained at 50 ˚C, thereafter as the leaching temperature increases the average surface area decreases. From inspection of results, a strong relation between leaching time and temperature exists. In order to obtain the maximum silica specific surface area possible as the temperature increases the leaching period has to decrease in order to avoid extensively damaging the silica structure. Further inspection of the leaching results also indicates a possible parameter interaction between acid concentration and leaching temperature. This interaction is confirmed with the statistically significant regression coefficient. The parameter interaction dictates for maximum silica SSA values as the AC increases the T has to decrease in order to avoid extensive damage to the silica backbone, this confirms observation obtained in literature (Section 2.9).

6. Conclusions and Recommendations

Using the combined results of all the experiments the maximum silica specific surface area values are obtained between the following ranges:

- Acid concentration: 4.26 M – 8.40 M
- Nitrate Ratio: 0.64
- Leaching Time: 12 hrs
- Leaching temperature: 50 ˚C

Based on the overall combined results aqua regia provides mesoporous silica with the highest SSA values within the above mentioned ranges. The aim was to determine the conditions capable of providing mesoporous silica with the highest specific surface area values and therefore the aim has been met.

Taking singular experiments into considerations, with *aqua regia* as leaching agent the maximum specific surface area of silica achieved is 515 m^2/g at acid concentration of 8.40 M, nitrate ratio of 0.64, leaching time of 12 hrs and leaching temperature at 50 ˚C. This experiment provided mesoporous silica with average pore width of 2.62 nm and average pore volume of 0.36 cm^3/g. The mesoporous silica obtained is 99.40% pure SiO_2 with trace amounts of MgO, Fe_2O_3 and TiO_2. Similar surface area values can be achieved with nitric acid at acid concentration of 6.33 M, leaching time of 6 hrs and leaching temperature at 60 ˚C. Nitric acid was able of providing sufficiently high surface area values at lower acid concentrations, shorter leaching times however at higher leaching temperatures. The same specific surface area values can be obtained by using either *aqua regia* or nitric acid as leaching agent. In general when using *aqua regia* the maximum surface area values are obtained at 12 hrs of leaching at nitrate ratio of 0.64, whereas with nitric acid, to obtained similar surface area values the optimal leaching temperature has to be at 60 ˚C.

Phlogopite is mined in copious amounts from the Phalaborwa complex and has little to no industrial use making it a low-cost and abundant raw material. With *aqua regia* as leachate in the above discussed experiments, approximately 17.6 % less nitric acid is needed at a lower temperature to achieve surface area

values in the range of 515 m^2/g. Interest in mesoporous silica utilization has greatly increased in areas such as catalysis, polymer reinforcement, adsorption and medical uses. These field have been rapidly expanding creating a need to finding more cost effective, time saving, environmentally friendly and economy growing process capable of providing the needed mesoporous high SSA silica. This study forms part of a larger study group focusing on the beneficiation of phlogopite. Not only is mesoporous silica recovered, valuable elements such as potassium, aluminum and magnesium are recovered. These elements are removed in forms of chlorides and nitrates and are widely used. Potassium chloride is used in fertilizer, medical areas and in food processing. Potassium nitrates are also used in fertilizer, gun powders and explosive. Magnesium chloride is used in water treatment, paper production, textile production and also in fire extinguishers. Magnesium nitrate is used in ceramics and paints. All of these products are used in multibillion rand industries yearly. All of the products recovered from the leaching process are in demand and contribute to the economic viability of the process.

A regression ($R^2 = 0.90$) was developed which can reasonably accurately estimate the specific surface area of the recovered silica with the acid concentration, nitrate ratio, leaching time and temperature.

It is recommended to further investigate the leaching capabilities of phlogopite in order to further increase the SSA. It is also recommended to investigate the possibility of increasing the size of the project to industrial scale, including budget estimation with economic and environmental impacts. It is also recommended to investigate changes in the structure of phlogopite when leached with nitric acid and *aqua regia* compared to when leached in hydrochloric acid. Nitric acid and *aqua regia* leached phlogopite has an amorphous structure whereas hydrochloric acid leached phlogopite retains its crystalline structure. It is also recommended to test the absorption properties of the recovered silica for purposes of metal removal from waste water streams.

7. References

Aitta, E, Lajunen, L and Leskela, M (1982) "A thermal study of the precipitates formed in ammonia neutralization of acidic solutions of dissolved Phlogopite" *Journal of Thermal Analysis,* 25 (1982), 117 – 125.

Akhaven, AC (2014) The Quartz Page, http://www.quartzpage.de/gen_mod.html

Aqua Regia Decomposition (2014) Arizona Gold Prospectors http://www.arizonagoldprospectors.com/Aquaregia.htm [2014, September 4].

Del Rey-Perez-Caballero, F and Poncelet, G (2000) "Preparation and characterization of microporous 18 Å Al-pillared structure from natural phlogopite micas" *Microporous and Mesoporous Materials*, 41(2000), 169 – 181.

Exchange Rate (sa) http://www.bloomberg.com/quote/USDZAR.Curr [2016, February 1]

Foster, MD (1960) "Interpretation of the Composition of Trioctahedral Micas" United States Geological Survey , 354(B)

Habashi, F (2005) "A short history of hydrometallurgy" *Hydrometallurgy*, 79(2005), 15 – 22.

Harkonen, MA and Keishi, RL (1984) "Porosity and Surface Area of Acid - Leached Phlogopite: The effect of leaching conditions and thermal treatment" *Colloids and Surfaces,* 11(1984), 323 – 339.

Hydrometallurgy Theory and Practice (2006) Murdock University, Mineral Council of Australia.

Iler, RK (1979) *The Chemistry of Silica*, Wiley – Interscience Publication, New York

Jordan, A (*sa*) Phyllosilicates http://gsoil.wordpress.com/tag/soil-genesis/ [2014, September 23].

Kaviratna, H and Pinnavaia, TM (1994) "Acid Hydrolysis of Octahedral Mg sites in 2:1 layered silicates: an assessment of the edge attack and the gallery access mechanisms" *Clays and Clay Minerals*, 42(6), 717 – 723.

Kraevskaya, SN, Belomestnova, EN and Zhuravlev, GI (1985) "Glass crystalline materials based on Phlogopite" Lensovet Lenungrad Institute of Technology, Tomsk Polytechnical Institute, 9, 12 – 13.

Kuwahara, Y and Aoki, Y (1995) "Dissolution process of phlogopite in acid solutions" *Clays and Clay Minerals*, 43(1), 39 – 50.

Levenspiel, O (1999) *Chemical Reaction Engineering*, John Wiley & Sons, New York.

Lin, FC and Clemency, CV (1981) "Dossolution Kinetics of Phlogopite. 1. Closed System" *Clay and Clay Minerals*, 29(2), 101 – 106.

Malmstrom, M and Banwart (1997) "Biotite dissolution at 25 ˚C: The pH dependence of dissolution rate and stoichiometry" *Geochemical et Cosmochimica Acta*, 61(14), 2779 – 2799.

Mamy. J (1969) "Extraction of interlayer K from Phlogopite Specific Effects of cations role of Na and H concentrations in Extraction Solutions" *Clay and Clay Minerals*, 18, 157 – 163.

Montgomery, DC and Runger, GC (2007) Applied Statistics and Probability for Engineers, John Wiley and Sons Inc, United States of America

Nelson, SA (2011) Phyllosilicates (Micas, Chlorite, Talc and Serpentine) Mineralogy, Tulane University.

Nitrosyl chloride Material Safety Data Sheet (2008) https://www.mathesongas.com/pdfs/msds/MAT16750.pdf [2014, September 4].

Okada, K, Arimitsu, N, Kameshima, Y, Nakajima, A and MacKenzie, KJ (2006) "Solid acidity of 2:1 type clay minerals activated by selective leaching" *Applied Clay Science*, 31(2006), 185 – 193.

Patnaik, P (2007) A comprehensive Guide to the Hazardous Properties of Chemical Substances, John Wiley & Sons, New Jersey

Phlogopite Structure (*sa*) https://dl.sciencesocieties.org/publications/books/abstracts/sssabookseries/soilmineralogyw/431?access=0&view=article [2014, September 4].

Price of Hydrochloric Acid (sa) http://www.alibaba.com/showroom/price-of-hydrochloric-acid.html [2016, February 1]

Price of Nitric Acid (sa) http://www.alibaba.com/showroom/price-of-nitric-acid.html [2016, February 1]

Princeton University Aqua Regia (2014) http://web.princeton.edu/sites/ehs/labsafetymanual/cheminfo/aquaregia.htm [2014, September 4].

Ross, GJ and Rich CI (1973a) "Effect of particle size on potassium sorption by potassium – depleted phlogopite" *Clay and Clay Minerals*, 21, 83 – 87.

Ross, GJ and Rich, CI (1973b) "Effect of particle thickness on potassium exchange from phlogopite" *Clay and Clay Minerals*, 21, 77 – 81.

Roy, R (1990) "*A Primer on the Taguchi Method*" Competitive Manufacturing Series, New York

Skoog, DA, Holler, EJ and Crouch, SR (2007) *Principles of Instrumental Analysis*, Thomson Brooks Cole, Canada

Steward, DB and Simmons, WB (2015) "Silica minerals" Encyclopedia Britannica Online, http:/www.britnnica.com/science/silica-minerals [2015, July 1]

Tan, KH (2005) Soil Sampling, Preparation and Analysis, Boca Raton, Florida.

Webb, PA, Orr, C, Camp,RW, Olivier, JP and Yunes, YS (1997) *Analytical Methods in Fine Particle Technology*, Micromeritics Instrument Corporation, Norcross

Wypych, F, Adad, LB, Mattoso, N, Marangon, AAS, Schreiner, WH (2004) "Synthesis and characterization of disordered layered silica obtained by selective leaching of octahedral sheets from chrysotile and phlogopite structures" *Journal of Colloid and Interface Science,* 283(2005), 107 - 112